Visible-Light Assisted Dehydrogenation of Benzylamines Catalysed by a Standalone Ruthenium Complex.

Laura Ibáñez-Ibáñez,[a] Mario del Pico-Carranza,[b] Gregorio Guisado-Barrios[b] and José A. Mata[a*]*

[a]Institute of Advanced Materials (INAM), Universitat Jaume I, Avda. Vicent Sos Baynat s/n, 12071, Castellón (Spain).

E-mail: jmata@uji.es

[b]Instituto de Síntesis Química y Catálisis Homogénea (ISQCH), CSIC-Universidad de Zaragoza, 50009, Zaragoza (Spain).

E-mail: gguisado@unizar.es

Table of Contents

S1. General procedures

S1.1. Reagents and solvents

All reagents were purchased from commercial suppliers and used without further purification. Anhydrous solvents were dried using a Solvent Purification System (SPS M BRAUM) or purchased from commercial suppliers degassed and stored over molecular sieves. Solvents used in catalytic experiments were deoxygenated using the freeze-pump-thaw methodology and kept under an atmosphere of nitrogen.

S1.2. Instrumentation

Nuclear magnetic resonance (**NMR**) spectra were recorded on Bruker spectrometers operating at 300 or 400 MHz (^{1}H NMR) and 75 or 100 MHz (^{13}C{^{1}H} NMR), respectively, and referenced to $SiMe_4$ (δ in ppm and *J* in Hertz). NMR spectra were recorded at room temperature with the appropriate deuterated solvent. Electrospray mass spectra (ESI-MS) were recorded on a SYNAPT XS High-Definition Mass Spectrometer (Waters Corporation, Manchester, UK) equipped with an electrospray ionization (ESI) source. UV-visible absorption spectra were recorded on a Varian Cary 300 BIO spectrophotometer and a JASCO V-780 spectrophotometer using dry and degassed methanol. Emission spectra were recorded on a FluoTime300 on similar methanol solutions, and using 2-methyl-THF for the emission spectra at 77K for complex **I**. The photocatalytic reactions were carried out in a homemade photoreactor (see Figure S36). The setup has a magnetic stirrer, Schlenk flask connected to a bubbler filled with mineral oil, stirring bar and two Kessil PR160L-440 nm LED lamps. Molecular hydrogen was detected using an Agilent 990 Micro-GC gas chromatograph, using argon as carrier gas.

S2. Synthesis and characterization of ruthenium complexes

S2.1. Synthesis of ruthenium complex I

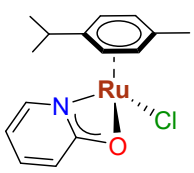

I

Synthesis of I. Metal complex **I** was prepared by modifying a reported method in the literature. [1] In a 30 mL Schlenk flask, under inert atmosphere, 2-hydroxypyridine (100 mg, 1.05 mmol) was dissolved in 5 mL of THF for 5 minutes. Then, solution was mixed with sodium hydride dry, 90% (30.3 mg, 1.2 eq.) and stirred for 30 min at room temperature using a bubbler filled with mineral oil to let the gas to be released from the reaction media. After that, solvent was eliminated by reduced pressure, forming a white precipitate that corresponds to the pyridone sodium salt (see Scheme 1). This salt was further reacted with [Ru(*p*-cymene)Cl_2]$_2$ (261.5 mg, 0.43 mmol) in 5 mL of dry CH_2Cl_2 during 3h at room temperature. Next, solution was filtered through a celite pad, precipitated in CH_2Cl_2/diethylether and dried under reduced pressure to obtain an orange solid (263 mg, 84% yield). ^{1}H NMR (400 MHz, $CDCl_3$): δ 7.85 (d, *J*= 7.4 Hz, 1H, CH_{Opy}), 7.31 (t, *J*= 5.9 Hz, 1H, CH_{Opy}), 6.41 (t, *J*= 5.9 Hz, 1H, CH_{Opy}), 6.05 (d, *J*= 8.6 Hz,1H, CH_{Opy}), 5.62 (dd, *J*= 5.8, 10.1 Hz, 2H, $CH_{p\text{-}cym}$), 5.37 (t, *J*= 5.8 Hz, 2H, $CH_{p\text{-}cym}$), 2.94 (m, 1H, CH_{iPr}), 2.35 (s, 3H, $CH_{3,Me}$), 1.33 (dd, *J*= 5.8, 10.1 Hz, 6H, $CH_{3,iPr}$). HRMS ESI-TOF-MS (positive mode): $[M\text{-}Cl]^+$ 330.0434; calc. 330.0436; ε_r: 0.6 ppm.

S2.2. Characterization NMR spectra of ruthenium complex I

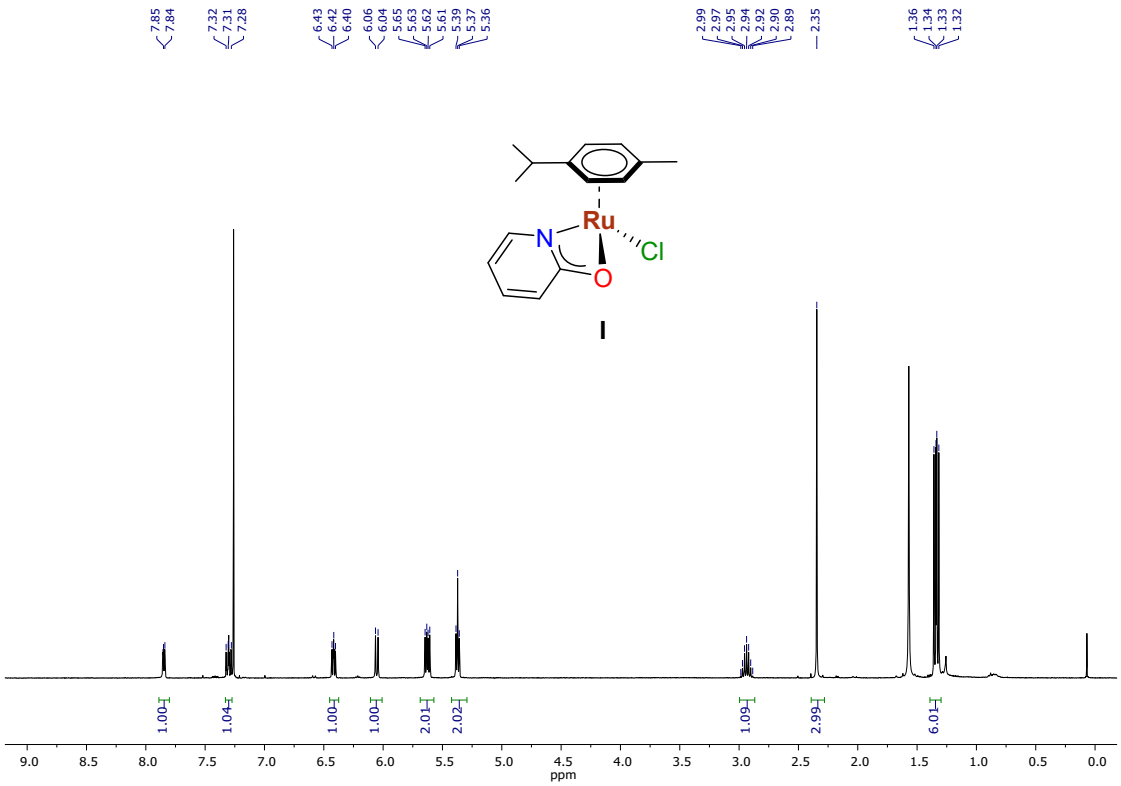

Figure S1 ^{1}H NMR spectrum of complex **I** in $CDCl_3$.

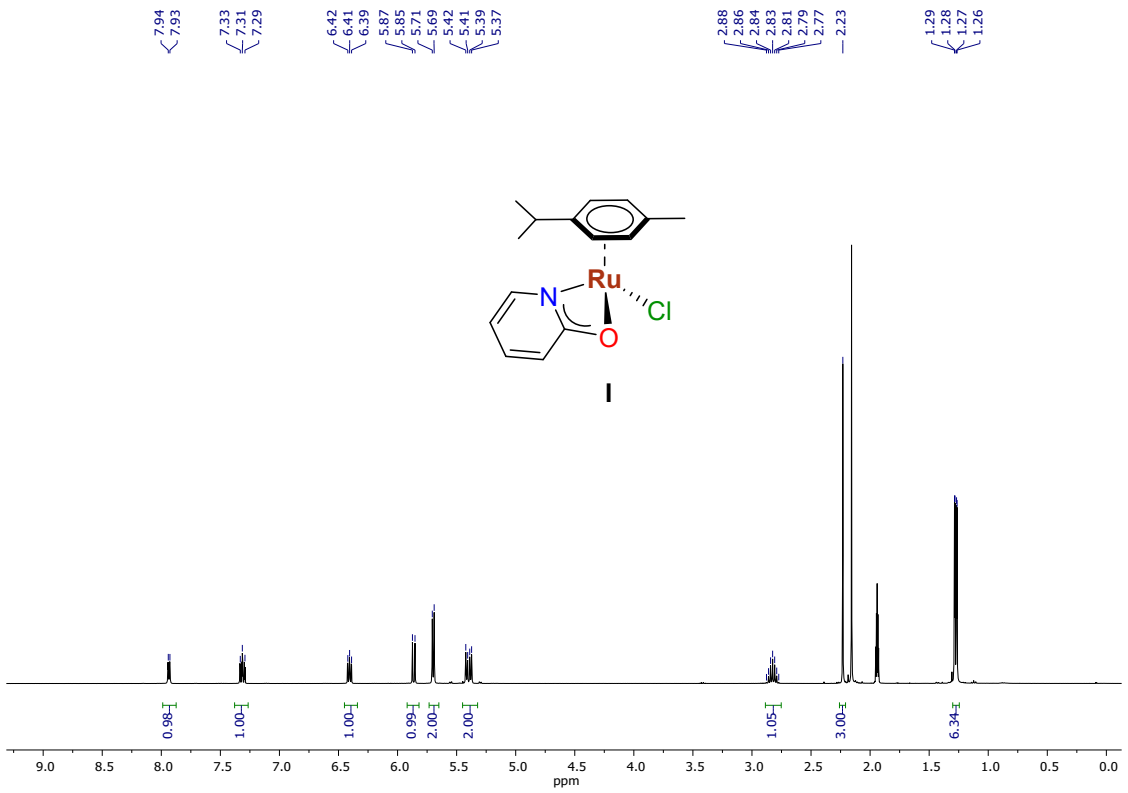

Figure S2 ^{1}H NMR spectrum of complex **I** in CD_3CN.

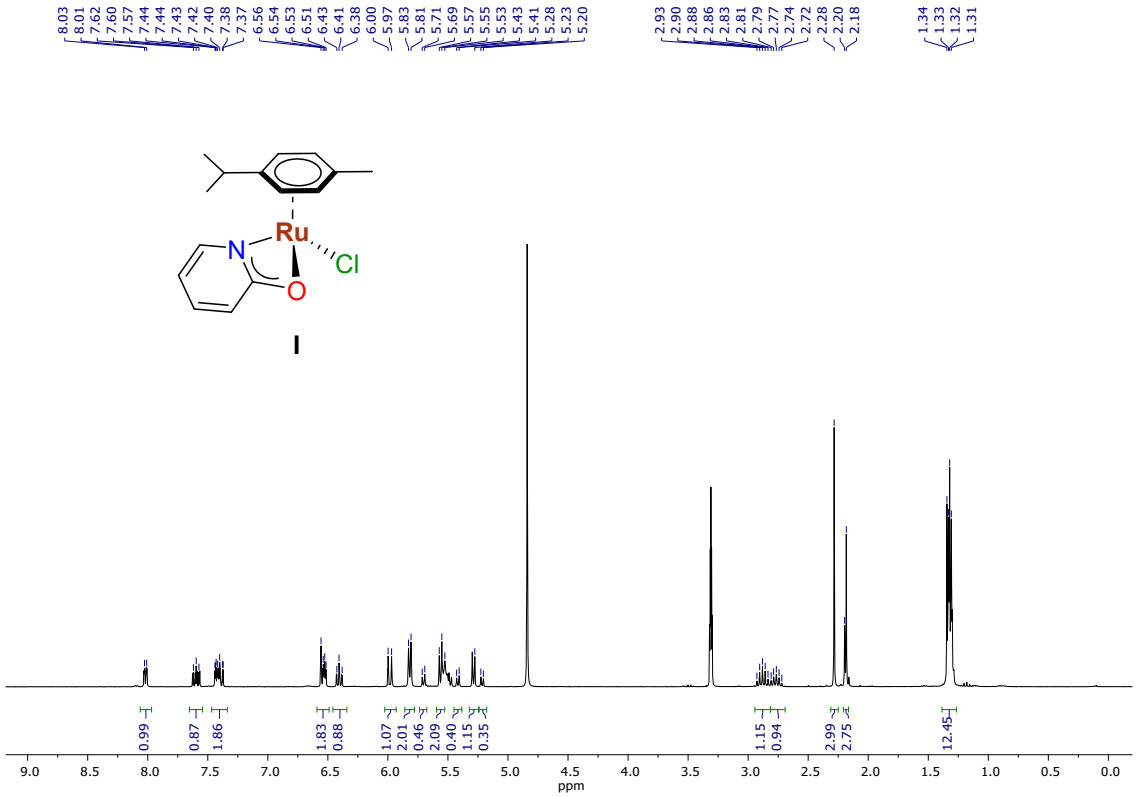

Figure S3 ^{1}H NMR spectrum of complex **I** in MeOD.

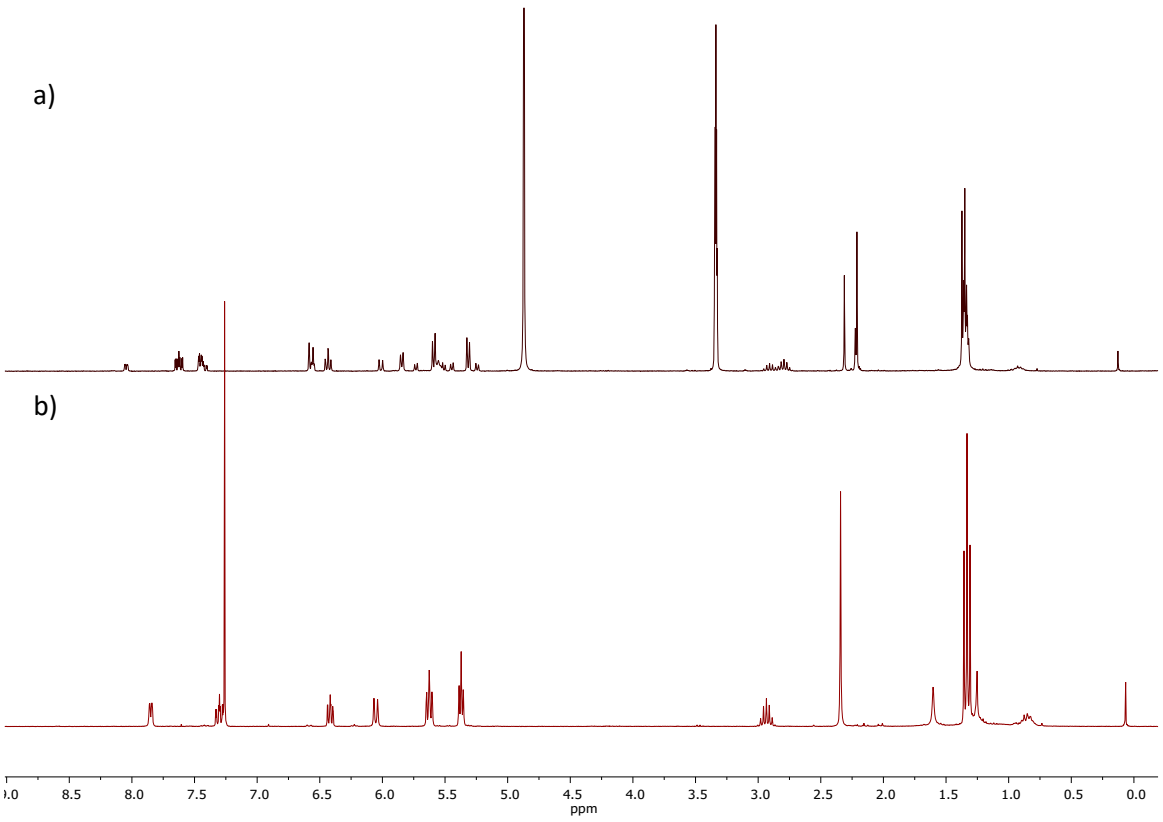

Figure S4 ^{1}H NMR of a) complex **I** in MeOD; b) **I** in $CDCl_3$ after MeOD solvent removal.

S2.3. HR-MS of ruthenium complex I

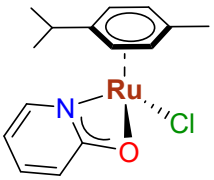

I

MW: 364.83 g/mol ($RuC_{15}H_{18}NOCl$)

Fragment: 330.0434 $[M - Cl]^+$, 270.9831 $[M - PyO]^+$

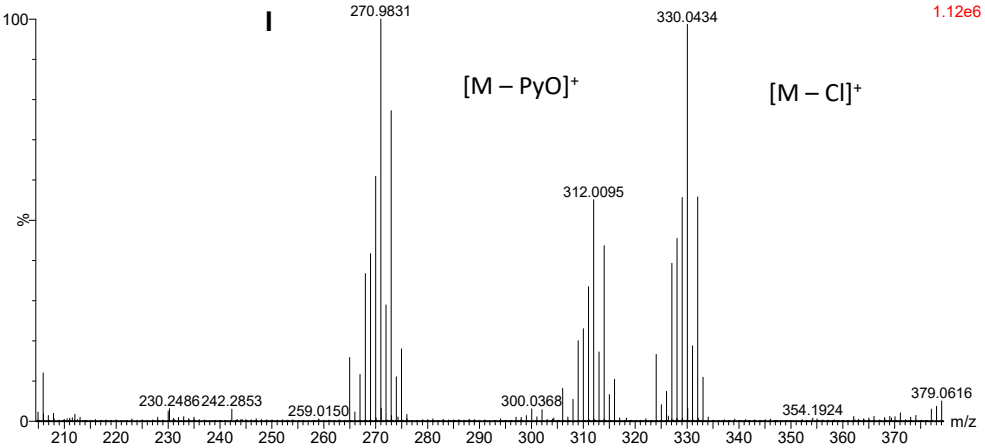

Figure S5 HR-MS of complex **I** in CH_3CN.

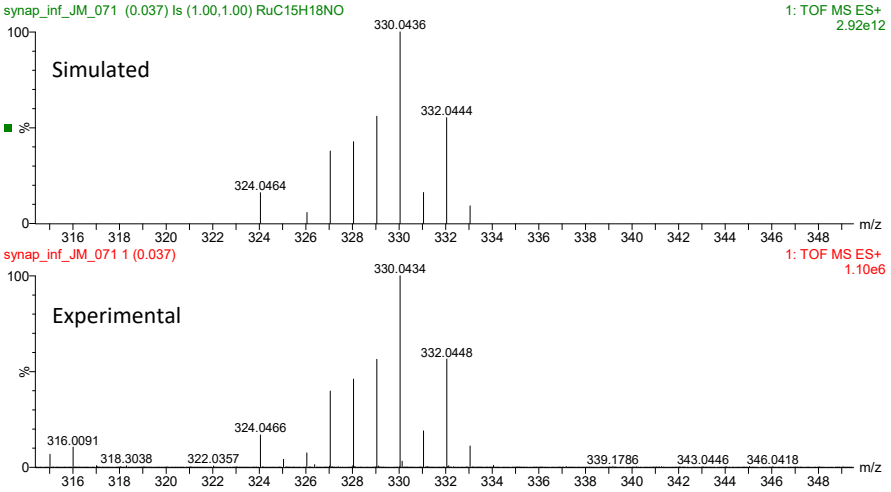

Figure S6 Comparison of simulated (top) and experimental (bottom) HRMS of complex **I**.

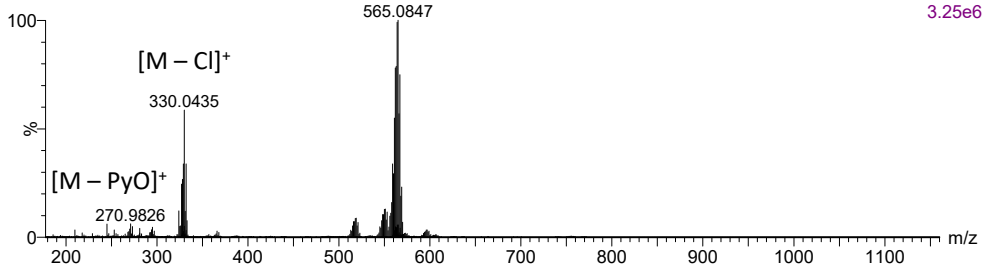

Figure S7 HR-MS of complex **I** in CH_3OH.

S2.4. Synthesis of ruthenium complexes II-VII

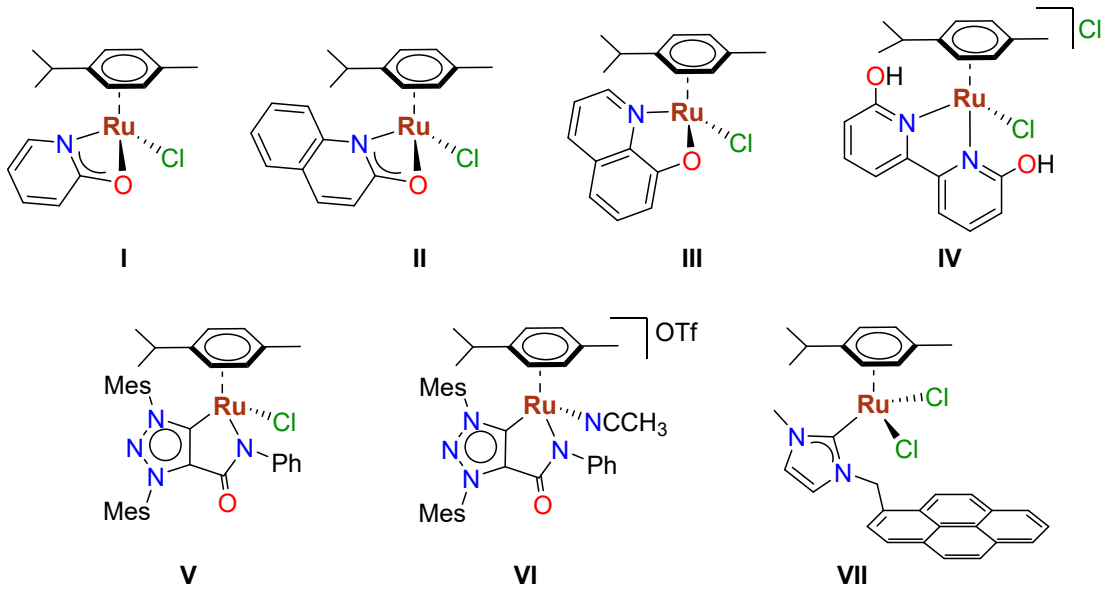

Figure S8 Ruthenium complexes **I-VII** used in photodehydrogenation of amines.

Ruthenium(II) complexes **II,**[2] **III**,[3] **IV** [4] and **VII** [5] were prepared according to reported procedures in the literature.

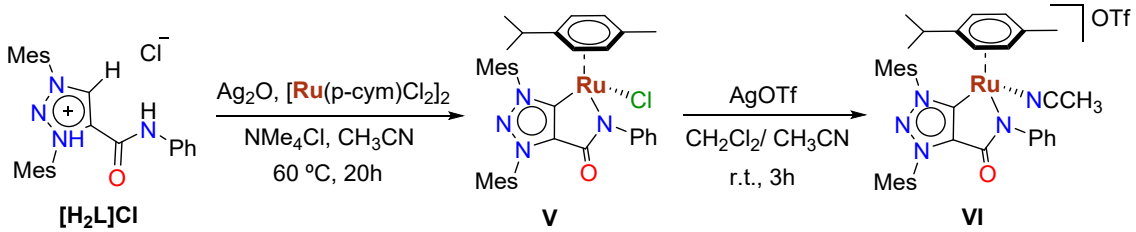

Scheme S1. Synthesis of neutral and cationic MIC-Ru^{II} complexes **V-VI**.

Synthesis of V. Metal complex **V** was prepared by adapting a reported method in the literature.[6]

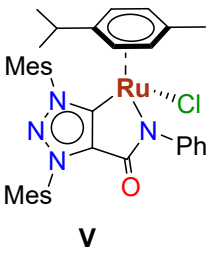

In a 100 mL Schlenk flask, under inert atmosphere, 1,3-dimesityl-4-(phenylcarbamoyl)-1H-1,2,3-triazol-3-ium chloride (200 mg, 0.43 mmol) $[H_2L]Cl$, Ag_2O (99 mg, 0.43mmol), $[Ru(p\text{-cymene})Cl_2]_2$ (132 mg, 0.21 mmol) and tetramethylammonium chloride (141 mg, 1,29 mmol) were introduced along with dry acetonitrile (8mL) and stirred for 20 hours at 60 °C in the absence of light, covered up in aluminum foil. The reaction mixture was filtered through celite and washed with acetonitrile (2 x 20 mL). Solvent was evaporated under reduced pressure. The resultant oil was redissolved in dichloromethane and filtered again through celite. Then, the solvent was partially removed, and the solution was passed through a silica gel chromatographic microcolumn, using DCM as eluent. The volatiles were removed under reduced pressure, to afford a brown solid. (247.4 mg, 83 % yield). ^{1}H NMR (400 MHz, CD_2Cl_2) δ 7.69 (dd, *J* = 8.5, 1.3 Hz, 2H, CH_{arom}), 7.24 (t, *J* = 7.8 Hz, 2H, CH_{arom}), 7.20 (d, *J* = 3.9 Hz, 2H, CH_{arom}), 7.05 (s, 1H, CH_{arom}), 7.04 – 6.99 (m, 1H, CH_{arom}), 6.99 (s, 1H, CH_{arom}), 5.22 (d, *J* = 6.3 Hz, 1H, $CH_{p\text{-cym}}$), 4.83 (d, *J* = 5.4 Hz, 1H, $CH_{p\text{-cym}}$), 4.72 (d, *J* = 6.3 Hz, 1H, $CH_{p\text{-cym}}$), 4.00 (d, *J* = 5.4 Hz, 1H, $CH_{p\text{-cym}}$), 2.47 (s, 3H, CH_3), 2.36 (s, 3H, CH_3), 2.32 (s, 3H, CH_3),

2.25 (s, 3H, CH_3), 2.25-2.18 (m, 1H, CH_{iPr}), 2.14 (s, 3H, CH_3), 1.92 (s, 3H, CH_3), 1.89 (s, 3H, CH_3), 0.94 (dd, *J* = 6.9, 1.8 Hz, 6H, C$H_{3,iPr}$). ^{13}C NMR (75 MHz, CD_2Cl_2) δ 171.8, 162.4, 153.8, 141.9, 141.5, 137.5, 135.8, 135.2, 134.3, 130.3, 129.6, 129.5, 129.4, 128.0, 127.6, 123.6, 100.7, 97.8, 95.0, 92.6, 81.7, 79.3, 31.1, 24.2, 21.6, 21.5, 21.1, 19.0, 18.9, 18.1, 17.8, 17.5. HRMS ESI-TOF-MS (positive mode): $[M+H]^+$ 695.2128; calc. 695.2097; ε_r: 4.4 ppm.

Synthesis of VI. Metal complex **VI** was synthesized following a reported method in the literature. [7] In a 100 mL Schlenk tube and under argon atmosphere, complex **V** (100 mg, 0.14 mmol) and AgOTf (37 mg, 0.144 mg) were added. Then, 15 mL of DCM and 2 mL of acetonitrile were introduced in the tube, and it was let stirring for 3 hours. The reaction crude was filtered through a celite pad, and the volatiles were removed under reduced pressure. The dark brown oil was redissolved in DCM (20 mL), filtered again through celite, and solvent was evaporated. The oil was precipitated with n-pentane and dried to afford a light brown powder. (121 mg, >99% yield).

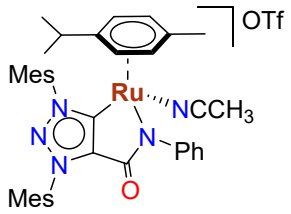

VI

^{1}H NMR (400 MHz, CD_2Cl_2) δ 7.41 (d, *J* = 7.5 Hz, 2H, CH_{arom}), 7.29 (t, *J* = 7.7 Hz, 2H, CH_{arom}), 7.22 (s, 2H, CH_{arom}), 7.13 – 7.06 (m, 2H, CH_{arom}), 6.99 (s, 1H, CH_{arom}), 5.79 (d, *J*= 6.4 Hz, 1H, C$H_{p\text{-}cym}$), 5.08 (d, *J* = 5.8 Hz, 1H, C$H_{p\text{-}cym}$), 4.84 (d, *J* = 6.4 Hz, 1H, C$H_{p\text{-}cym}$), 4.24 (d, *J* = 5.7 Hz, 1H, C$H_{p\text{-}cym}$), 2.42 (s, 6H, CH_3), 2.31 (s, 3H, CH_3), 2.18 (s, 3H, CH_3), 2.05 (s, 3H, CH_3), 2.03 (s, 3H, CH_3), 2.01 – 1.96 (m, 1H, CH_{iPr}), 1.87 (s, 3H, CH_3), 1.84 (s, 3H, CH_3), 0.87 (d, *J* = 7.0 Hz, 3H, $CH_{3,iPr}$), 0.83 (d, *J* = 6.9 Hz, 3H, $CH_{3,iPr}$).^{13}C NMR (75 MHz, CD_2Cl_2) δ 167.7, 163.0, 148.2, 143.3, 142.8, 135.1, 135.0, 134.4, 134.3, 130.9, 130.7, 130.1, 130.0, 129.9, 129.8, 127.0, 126.4, 124.5, 119.2, 105.4, 101.2, 96.7, 93.7, 84.8, 83.8, 31.3, 24.0, 21.7, 21.6, 21.0, 19.0, 18.2, 17.8, 17.2, 4.5. HRMS ESI-TOF-MS (positive mode): $[M - OTf - NCCH_3]^+$ 659.2347; calc. 659.2334; ε_r: 1.9 ppm.

S2.5. Characterization NMR spectra of ruthenium complexes II-VII

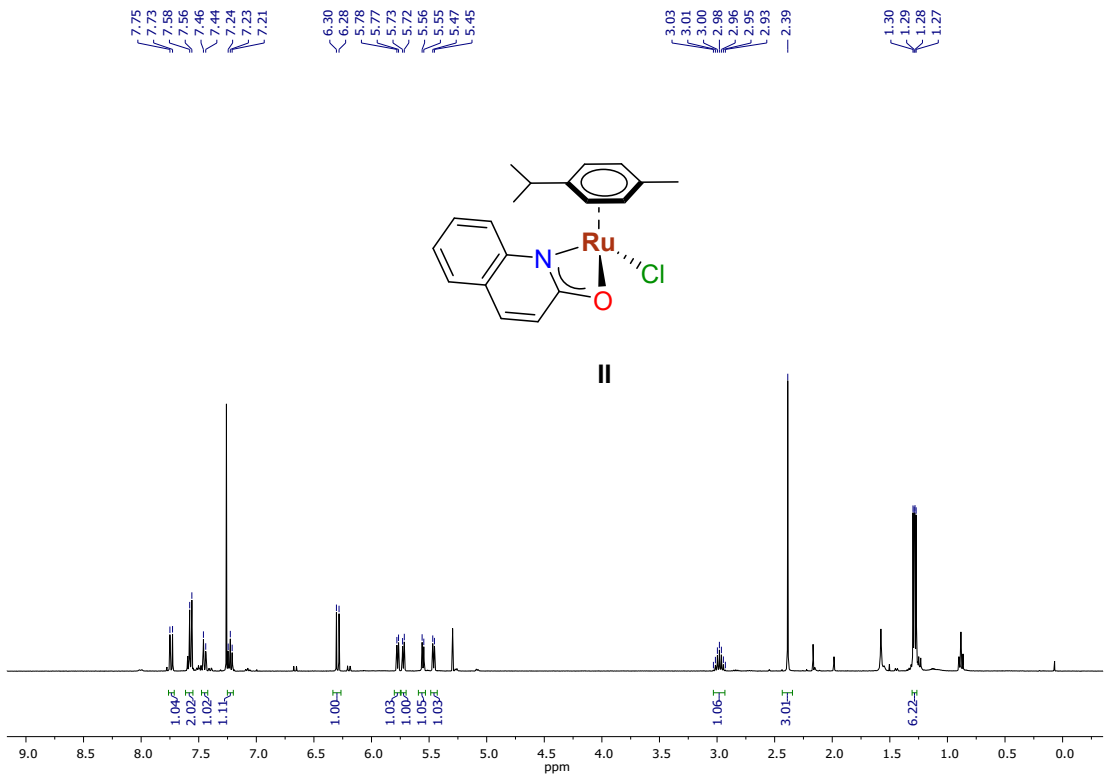

Figure S9 ^{1}H NMR spectrum of complex **II** in $CDCl_3$.

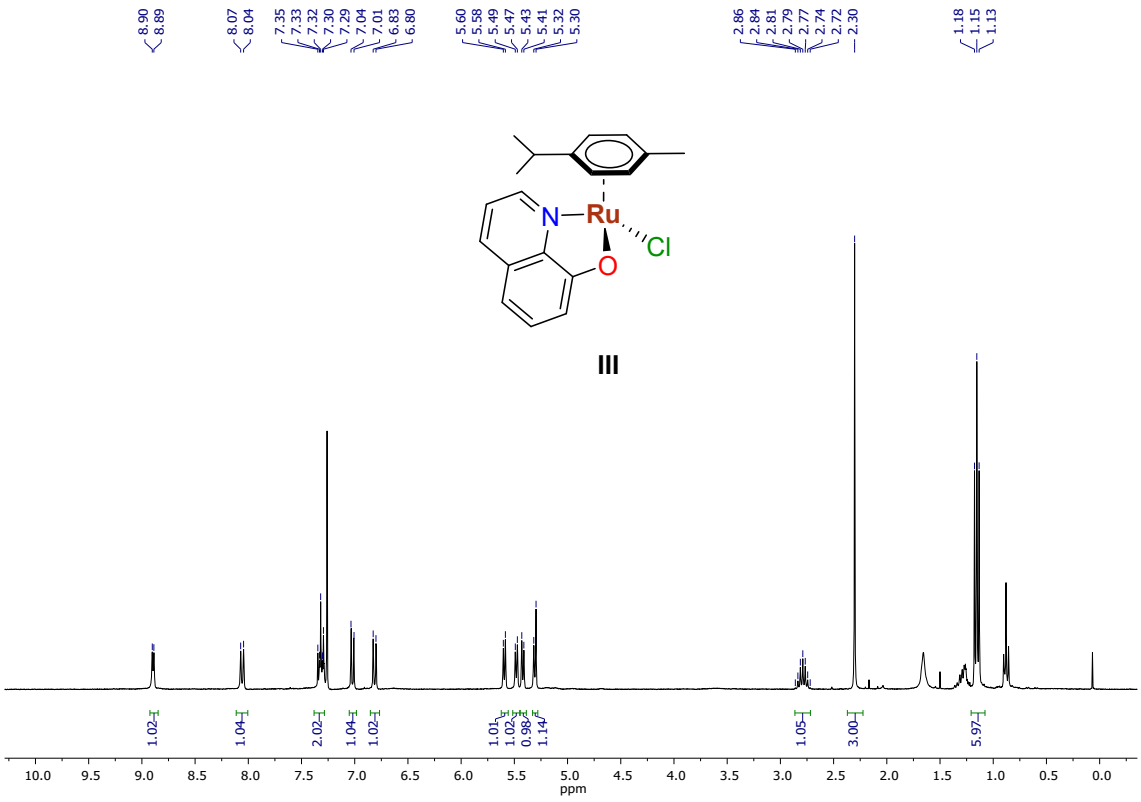

Figure S10 ^{1}H NMR spectrum of complex **III** in $CDCl_3$.

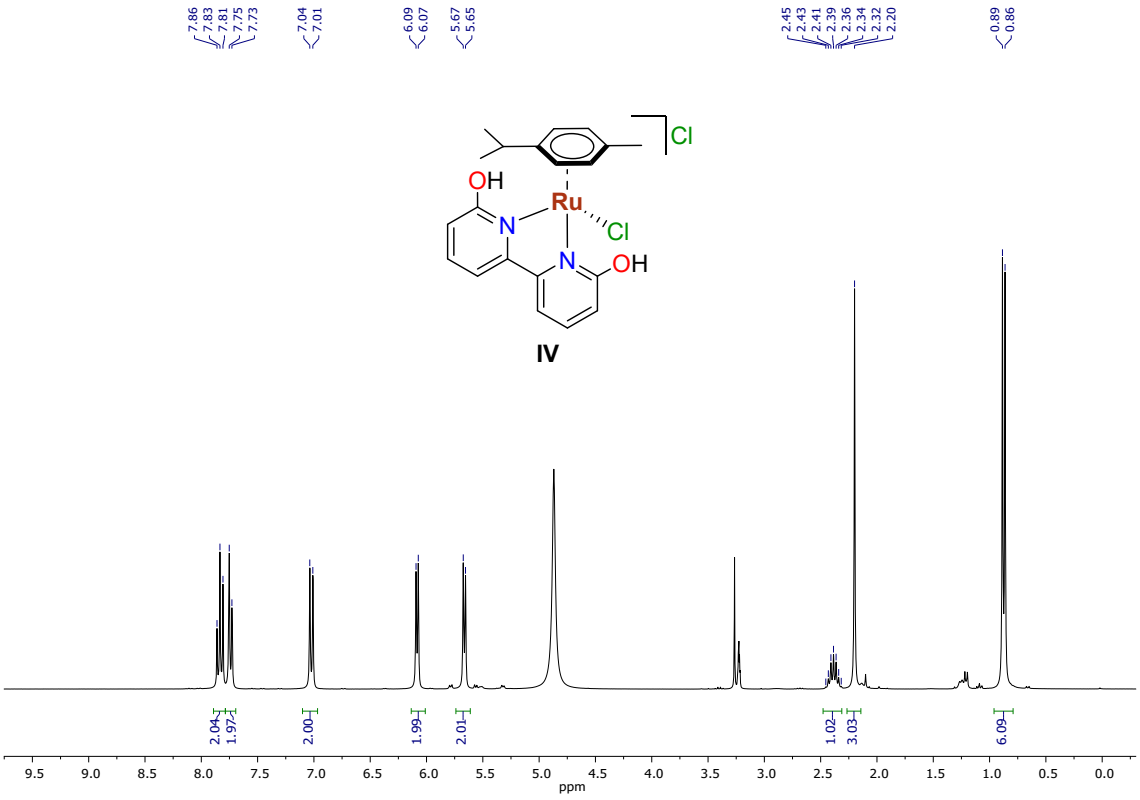

Figure S11 ^{1}H NMR spectrum of complex **IV** in MeOD.

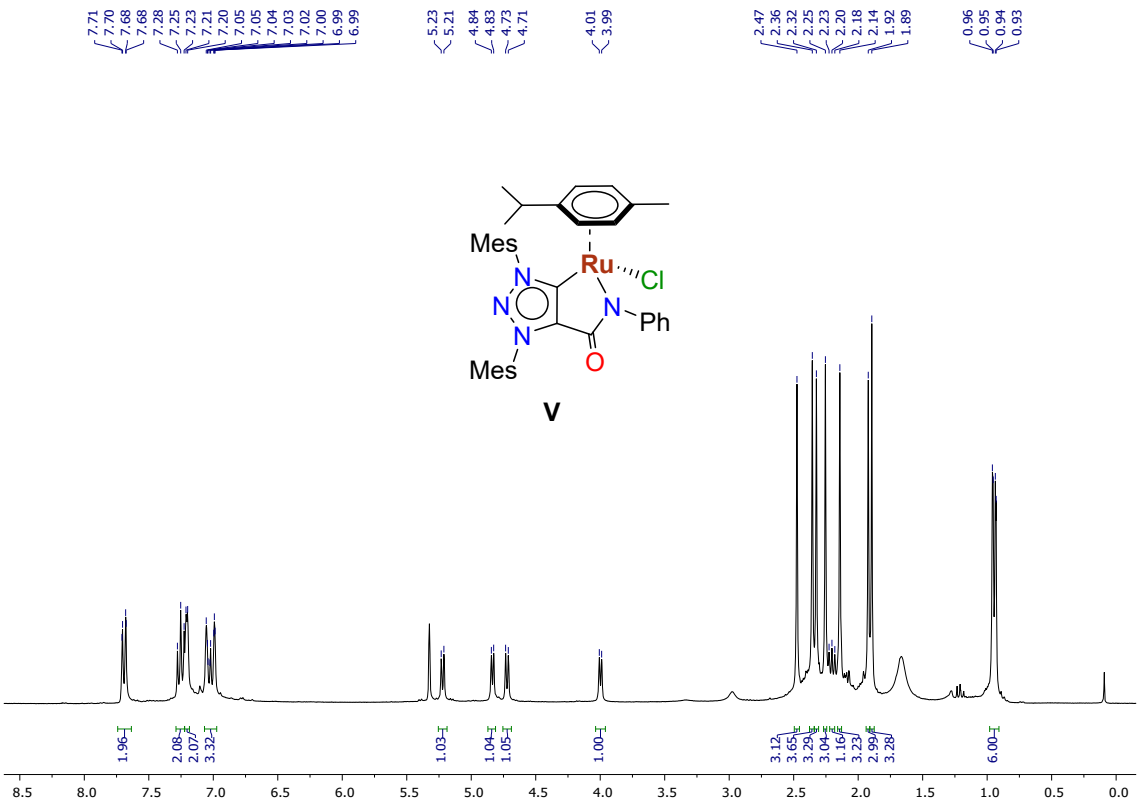

Figure S12 ^{1}H NMR spectrum of complex **V** in CD_2Cl_2.

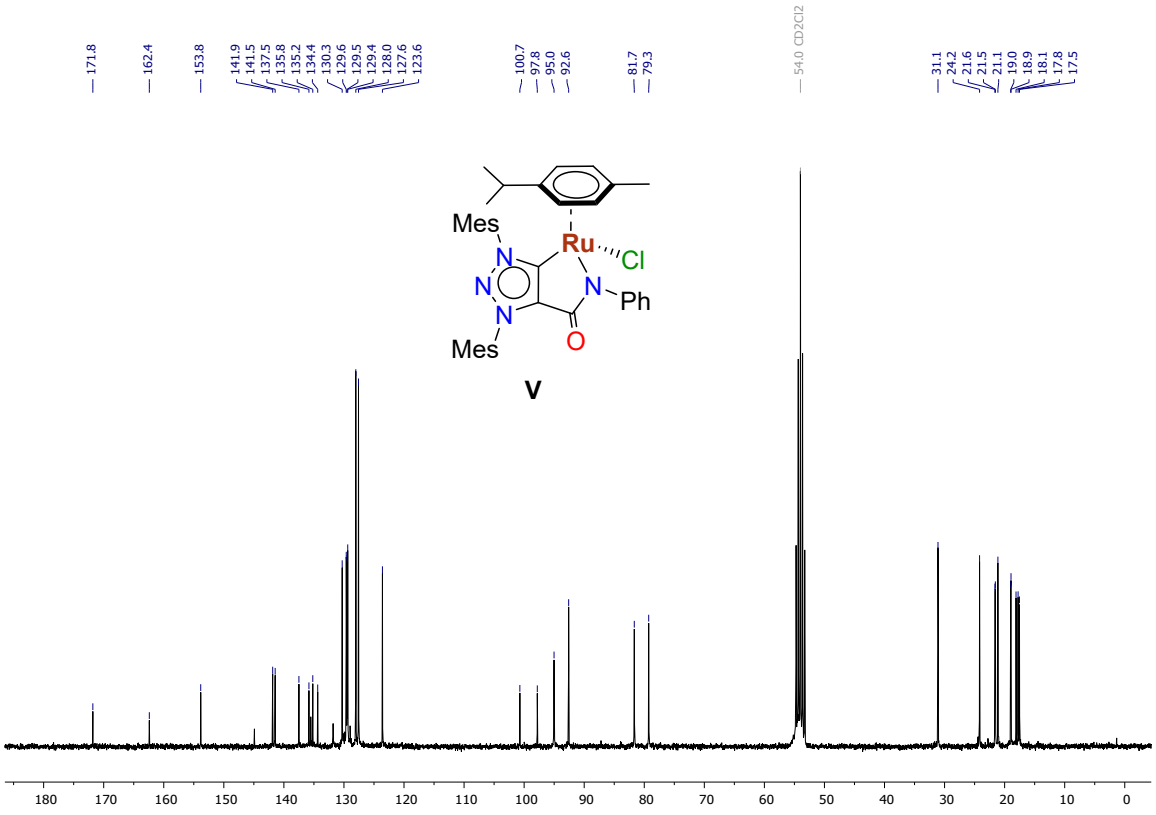

Figure S13 ^{13}C NMR spectrum of complex **V** in CD_2Cl_2.

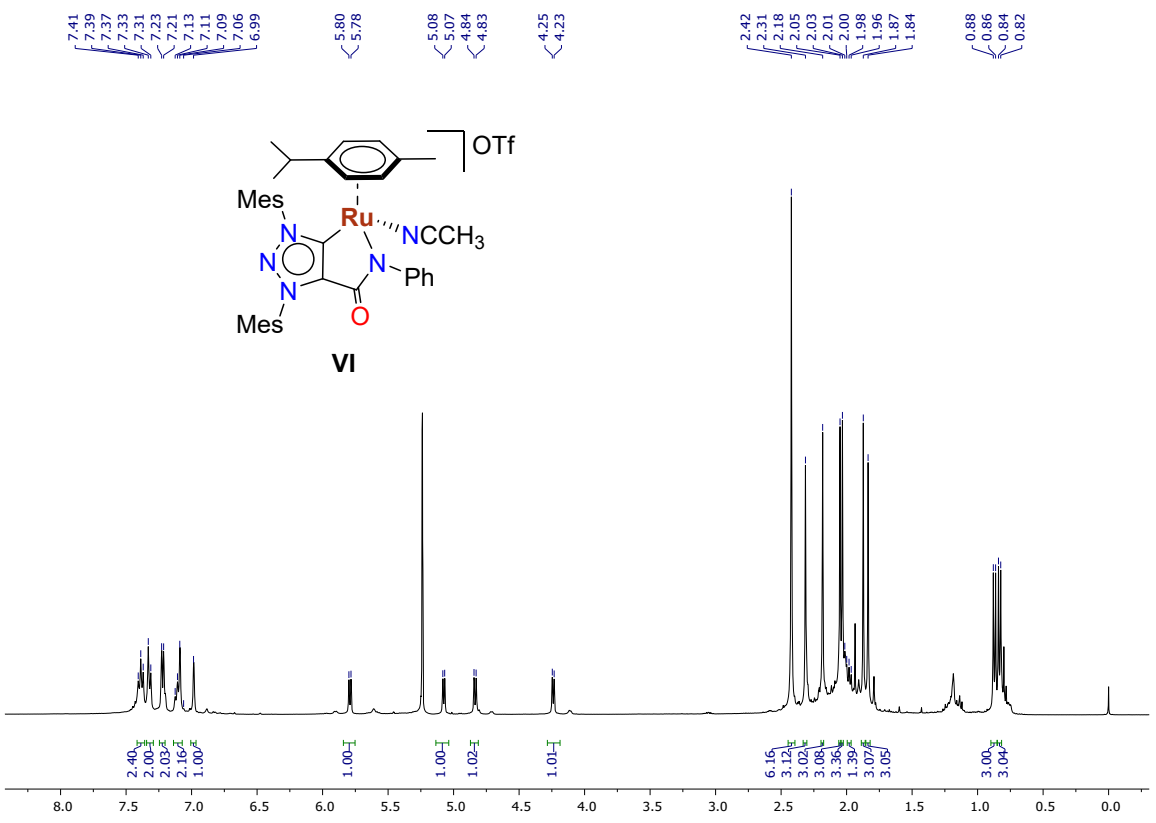

Figure S14 ^{1}H NMR spectrum of complex **VI** in CD_2Cl_2.

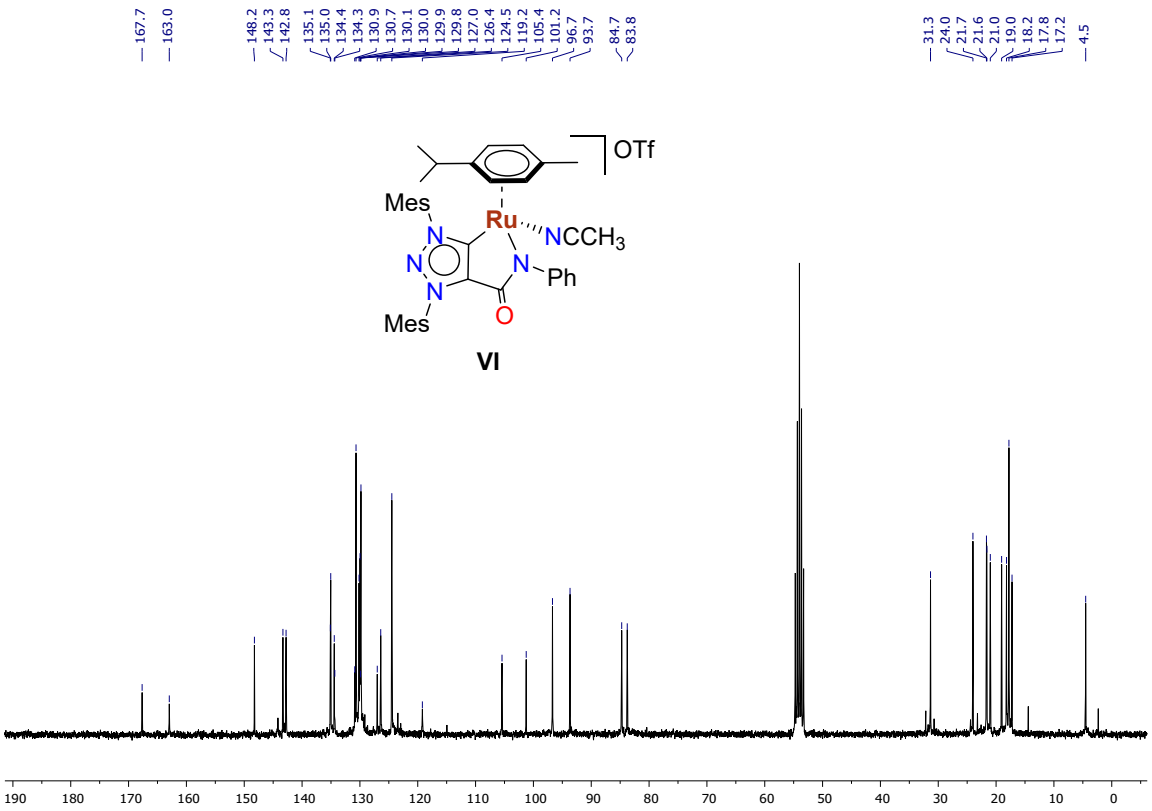

Figure S15 ^{13}C NMR spectrum of complex **VI** in CD_2Cl_2.

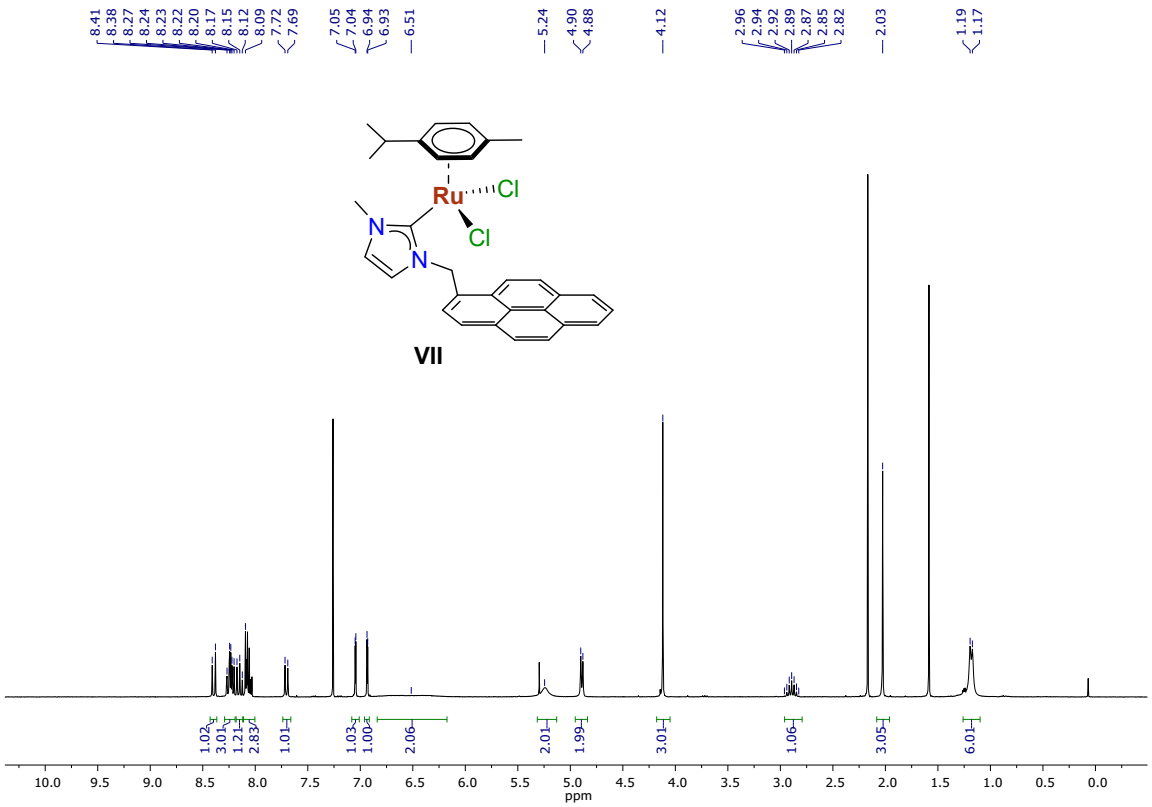

Figure S16 ^{1}H NMR spectrum of complex **VII** in $CDCl_3$.

S2.6. HR-MS of ruthenium complexes II – VII

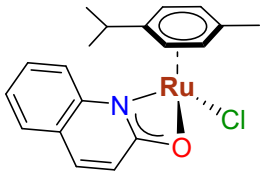

II

MW: 414.89 g/mol ($RuC_{19}H_{20}NOCl$)

Fragment: 380.0594 $[M - Cl]^+$

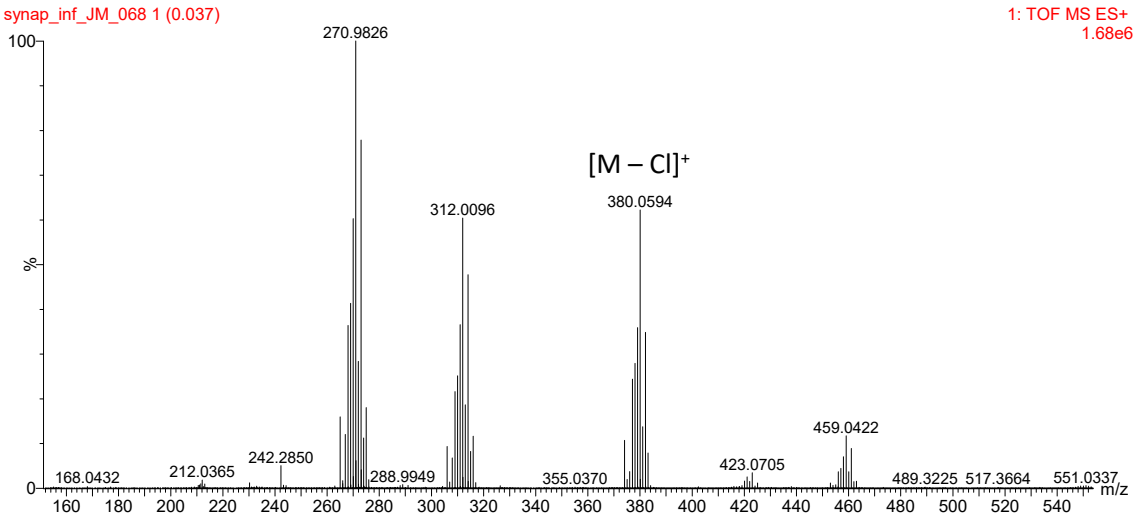

Figure S17 HR-MS of complex **II** in CH_3CN.

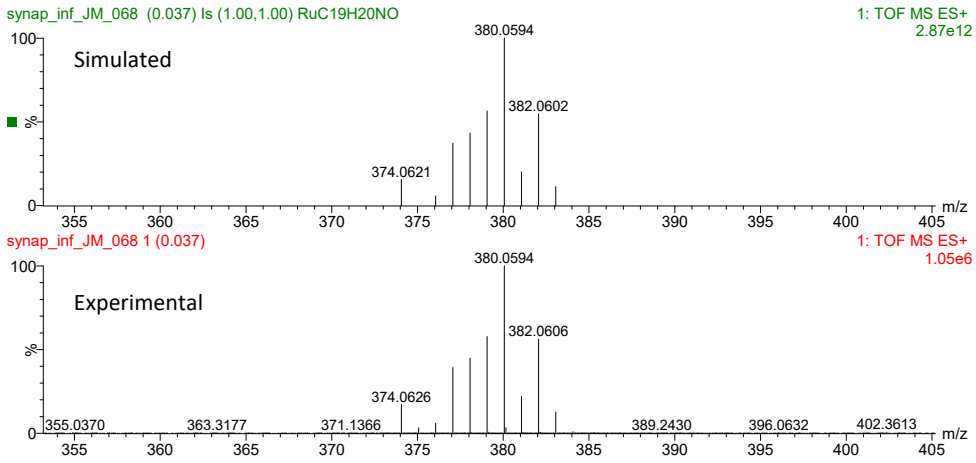

Figure S18 Comparison of simulated (top) and experimental (bottom) HR-MS of complex **II**.

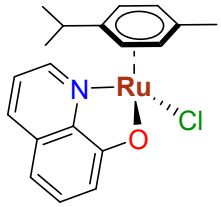

III

MW: 414.89 g/mol ($RuC_{19}H_{20}NOCl$)

Fragment: 380.0597 $[M - Cl]^+$

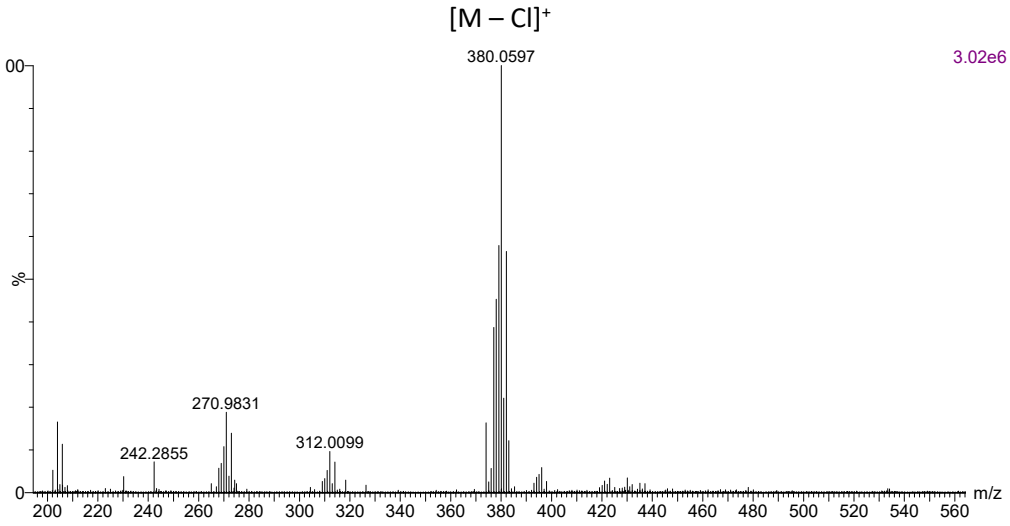

Figure S19 HR-MS of complex **III** in CH_3CN.

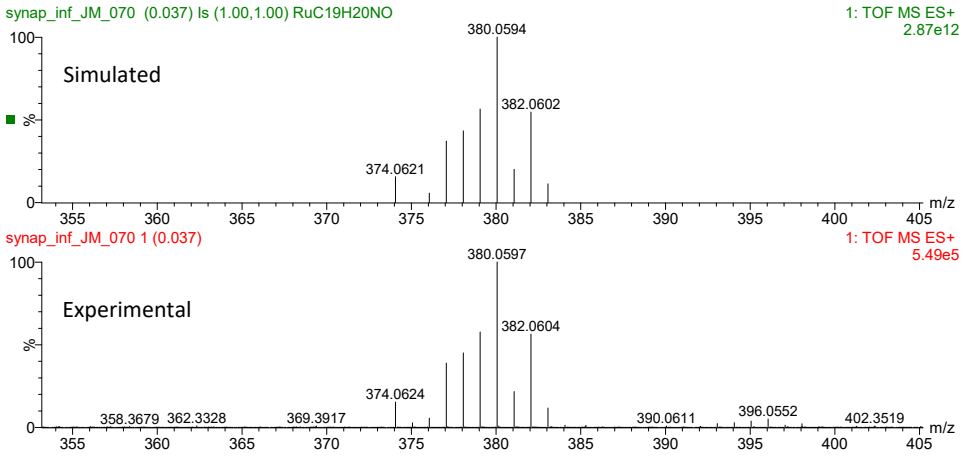

Figure S20 Comparison of experimental (top) and simulated (bottom) HR-MS of complex **III**.

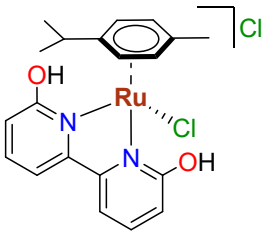

IV

MW: 494.38 g/mol ($RuC_{20}H_{22}N_2O_2Cl_2$)

Fragments: 459.0421 $[M - Cl]^+$

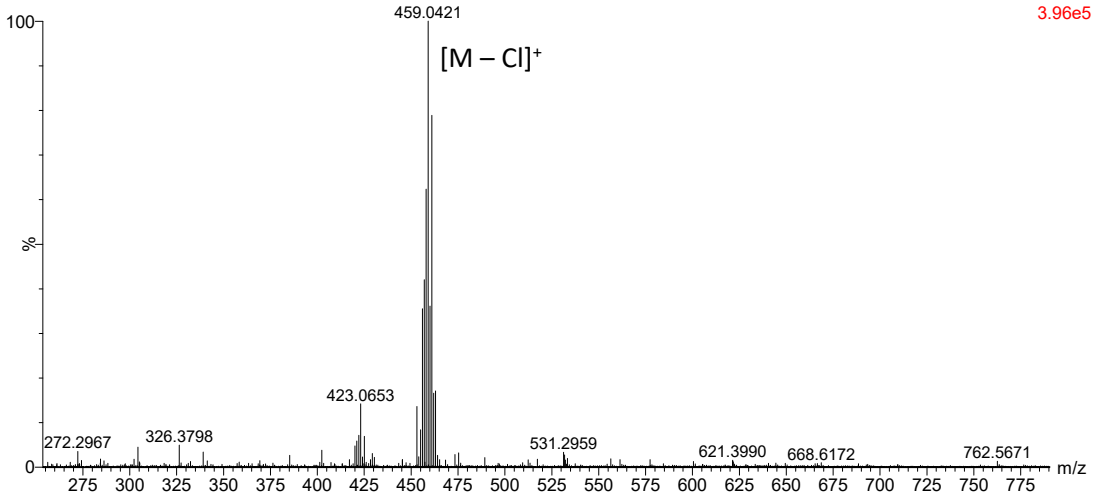

Figure S21 HR-MS of complex **IV** in CH_3OH.

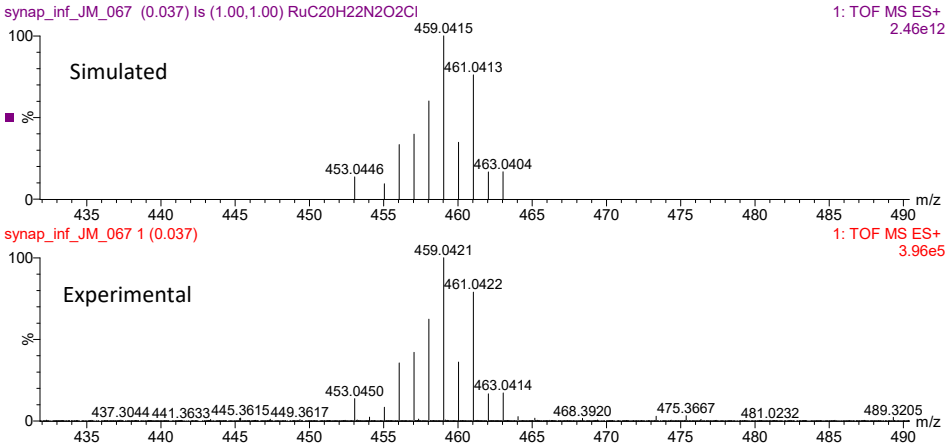

Figure S22 Comparison of simulated (top) and experimental (bottom) HR-MS of complex **IV**.

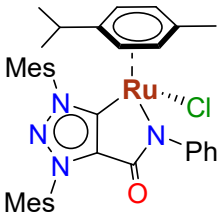

V

MW: 694.25 g/mol ($RuC_{37}H_{41}N_4OCl$)

Fragment: 695.2128 $[M + H]^+$

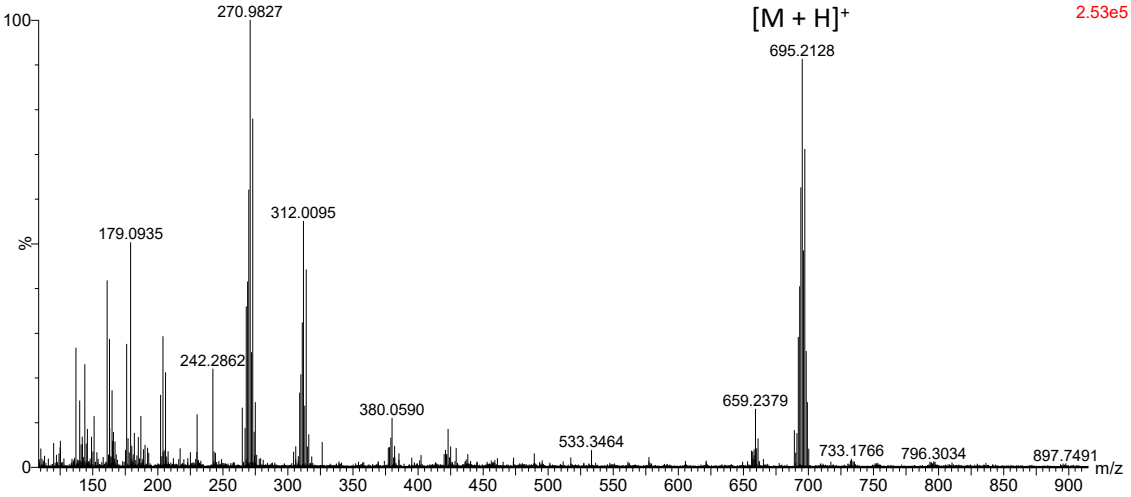

Figure S23 HR-MS of complex **V** in CH_3CN.

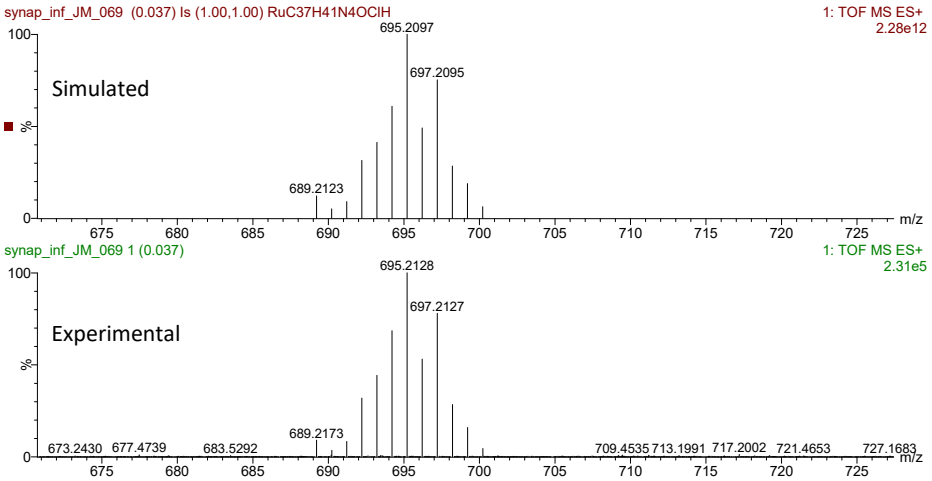

Figure S24 Comparison of simulated (top) and experimental (bottom) HR-MS of complex **V**.

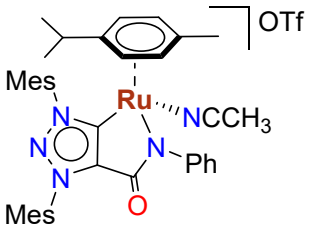

VI

MW: 848.91 g/mol ($[RuC_{39}H_{44}N_5O]CF_3SO_3$)

Fragment: 659.2347 $[M - OTf - MeCN]^+$

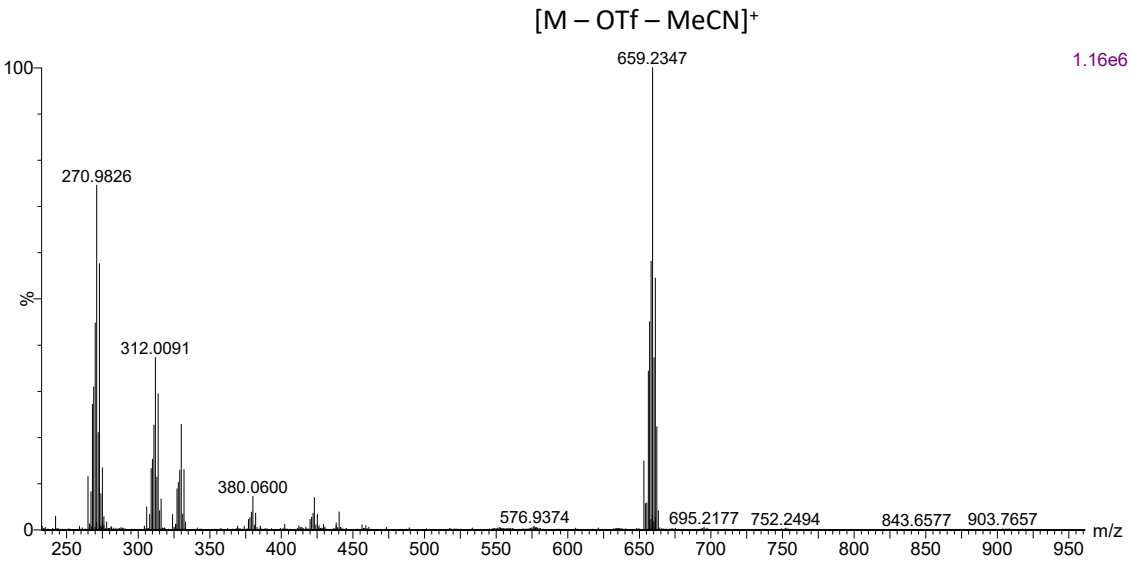

Figure S25 HR-MS of complex **VI** in CH_3CN.

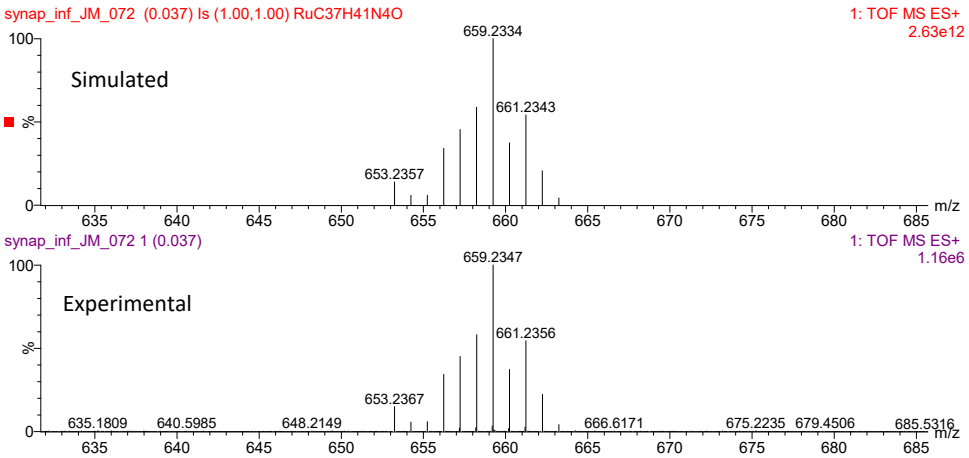

Figure S26 Comparison of simulated (top) and experimental (bottom) HR-MS of complex **VI**.

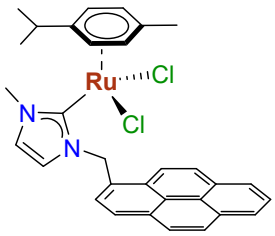

VII

MW: 602.57 g/mol ($RuC_{31}H_{30}Cl_2N_2$)

Fragment: 567.1151 $[M - Cl]^+$

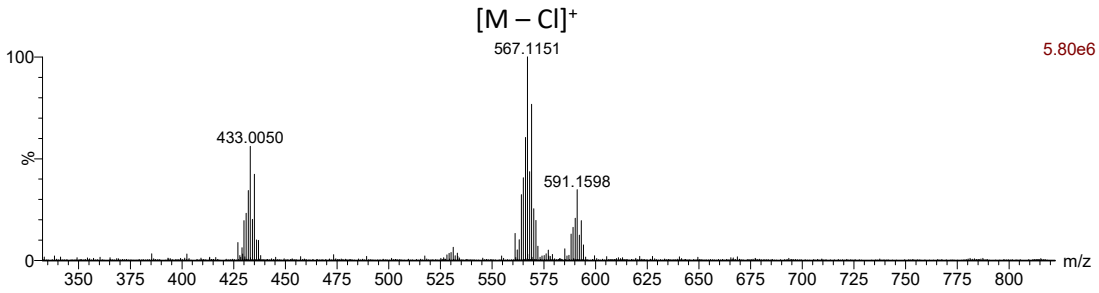

Figure S27 HR-MS of complex **VII** in CH_3CN.

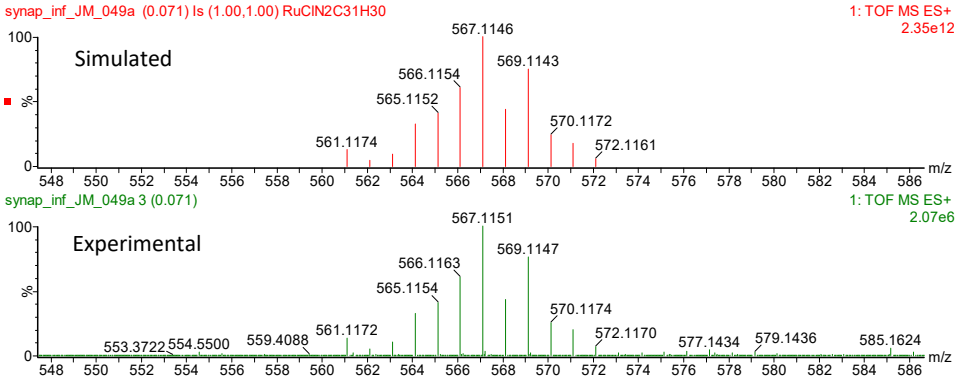

Figure S28 Comparison of simulated (top) and experimental (bottom) HR-MS of complex **VII**.

S2.7. Absorption spectra of ruthenium complexes I-VII

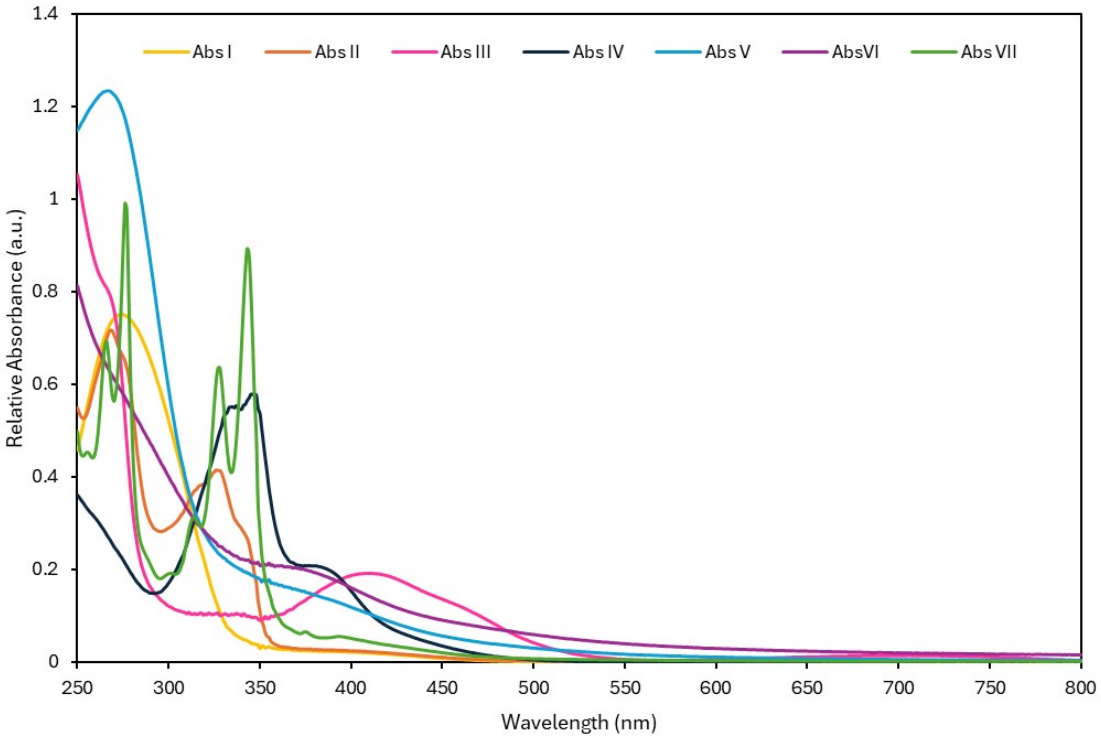

Figure S29 Absorption spectra of complexes **I-VII** in degassed methanol (5.0 x 10^{-5} M).

S2.8. Absorption and emission of ruthenium complex I

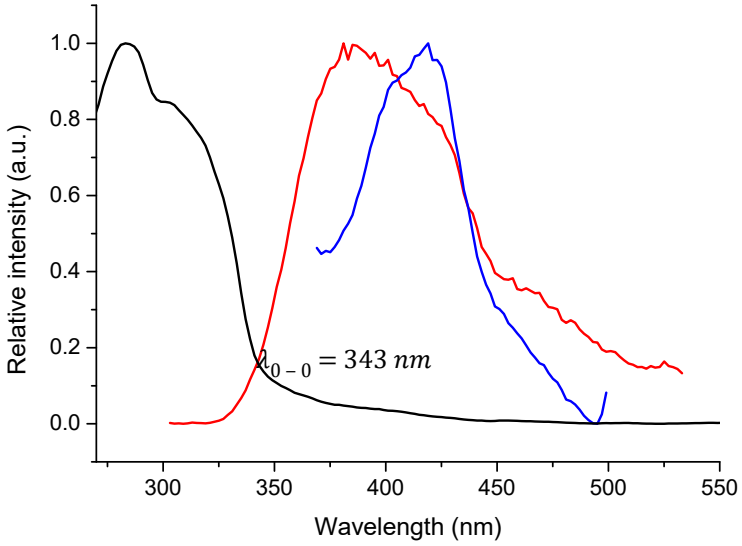

Figure S30 Absorption of complex **I** (black) and emission spectra at 298K (red) and 77K (blue)**.** Solutions were prepared in dry MeOH (absorption and emission at 298 K) or dry 2-methyl-THF (emission at 77K), 1mM. The energy associated with $\lambda_{0\text{-}0}$ is $E_{0\text{-}0}$ = 3.6 eV.

S2.9. Cyclic voltammetry of ruthenium complex I

Cyclic voltammetry (CV) experiments were performed using a standard three-electrode configuration consisting of a glassy carbon disk working electrode, a silver (Ag/AgCl) reference electrode, and a platinum counter electrode. The electrolyte solution was prepared by dissolving ([^{n}Bu$_4$N][PF$_6$], 0.1 M) in anhydrous acetonitrile (MeCN). A volume of 5 mL of the supporting electrolyte solution was transferred to the electrochemical cell under an inert atmosphere. The analyte was added directly to the electrolyte to achieve a final concentration of 3 mM. When applicable, ferrocene (Fc) was added as an internal standard at a concentration of 3 mM. Prior to measurements, the solution was thoroughly degassed with argon for at least 5 minutes to remove dissolved oxygen. During voltammetry, a gentle positive pressure of inert gas was maintained over the solution. Voltammograms were recorded in the potential range of –2.4 to +2 V vs Ag, at a scan rate of 50 mV/s, unless otherwise stated. Under these conditions, ferrocene exhibited a reversible redox couple centered at approximately +0.4 V vs Ag, consistent with literature values in MeCN. Redox potentials of analytes were reported recalibrated to the Fc/Fc$^+$ couple. Control experiments on blank electrolyte solutions (0.1 M [^{n}Bu$_4$N][PF$_6$] in MeCN) were conducted to monitor for residual moisture or oxygen. All measurements were performed at room temperature (~20 °C).

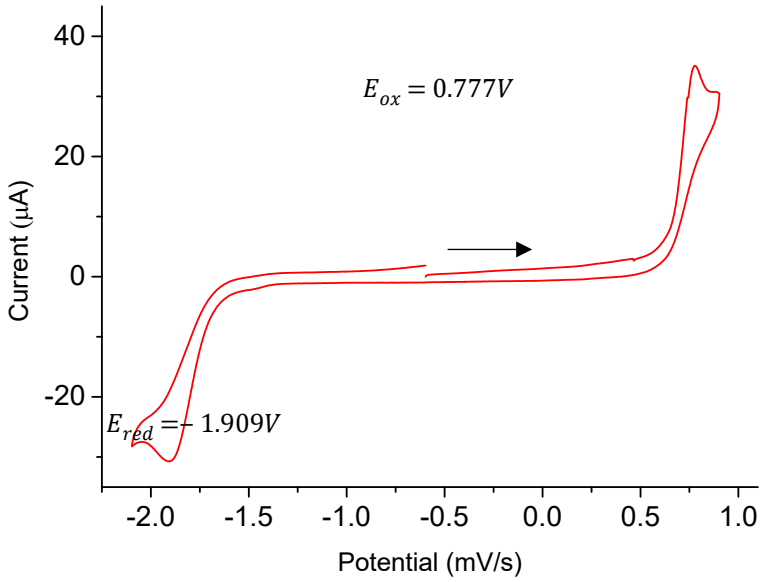

Figure S31 Cyclic voltammetry performed on a 3 x 10^{-3} M solution of ruthenium complex **I** at a scan rate of 100 mV/s.

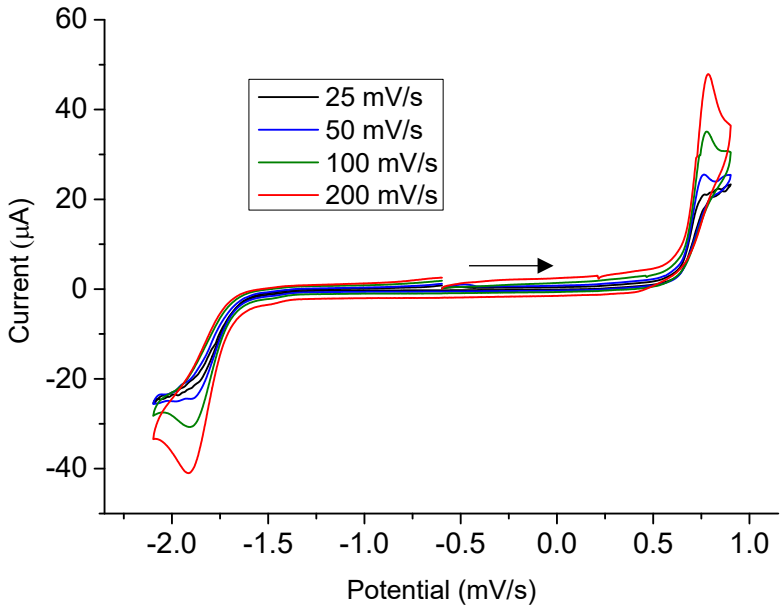

Figure S32 Cyclic voltammetry performed on a 3 x 10^{-3} M solution of ruthenium complex **I** at different scan rates.

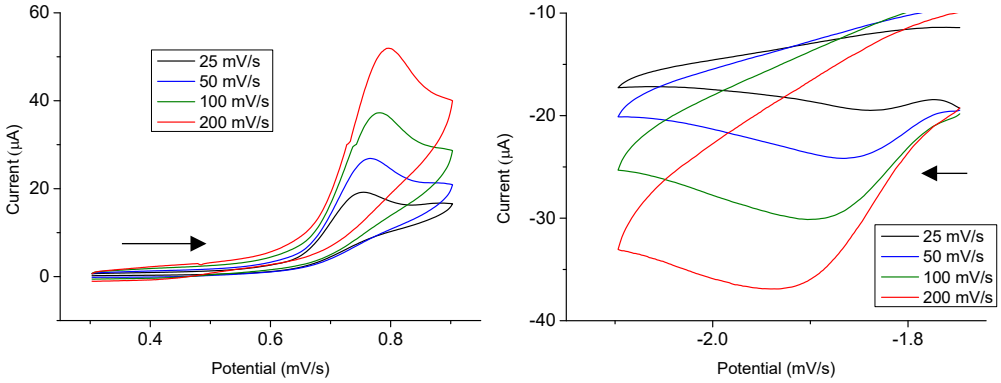

Figure S33 Cyclic voltammetry performed on a 3 x 10^{-3} M solution of ruthenium complex **I** at different scan rates, focusing on the oxidation (left) and reduction (right) processes

With these data, and using the Rehm-Weller equation, the redox potentials in the excited state of complex **I** were estimated.

$$E^*_{red} = E_{red} + E_{0-0} \qquad E^*_{ox} = E_{ox} - E_{0-0}$$

The excited state redox potential for the reduction process turned to be E^*_{red} = 1.691 V and E^*_{ox} = -2.823 V vs Fc/Fc^+

S2.10. Synthesis and characterization of complex VIII

Synthesis of VIII. Metal complex **VIII** was synthesized by mixing complex **I** (25 mg, 0.069 mmol), and AgOTf (26.7 mg, 1.5 eq.) in 2 mL of DCM and 1 mL of CH_3CN

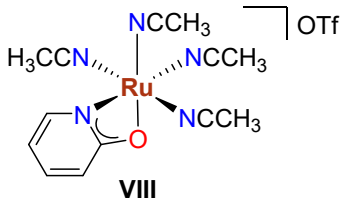

VIII

in a Schlenk flask under inert atmosphere. Solution was stirred at reflux overnight. After that, a brown solution was obtained, which was filtrated in celite and washed with acetonitrile (2 x 10 mL). Volatiles were removed under reduced pressure, obtaining a brown oil. The oil was washed with diethylether and chloroform to eliminate free *p*-cymene, and dried under reduced pressure, obtaining a brown solid (20 mg, 57% yield). ^{1}H NMR (300 MHz, CD_3OD) δ 8.28 (d, *J* = 6.1 Hz, 1H, CH_{Opy}), 7.79 (t, *J* = 6.9 Hz, 1H, CH_{Opy}), 6.99 (t, *J* = 6.5 Hz, 1H, CH_{Opy}), 6.85 (d, *J* = 8.3 Hz, 1H, CH_{Opy}), 2.63 (s, 3H, CH_3), 2.57 (s, 9H, CH_3). ^{13}C NMR (100 MHz, CD_3OD) δ 169.6, 154.2, 117.9, 112.2, 2.9. HRMS ESI-TOF-MS (positive mode): $[M - OTf - NCCH_3]^+$ 319.0143; calc. 319.0136; ε_r: 2.2 ppm.

NMR Spectra of complex VIII

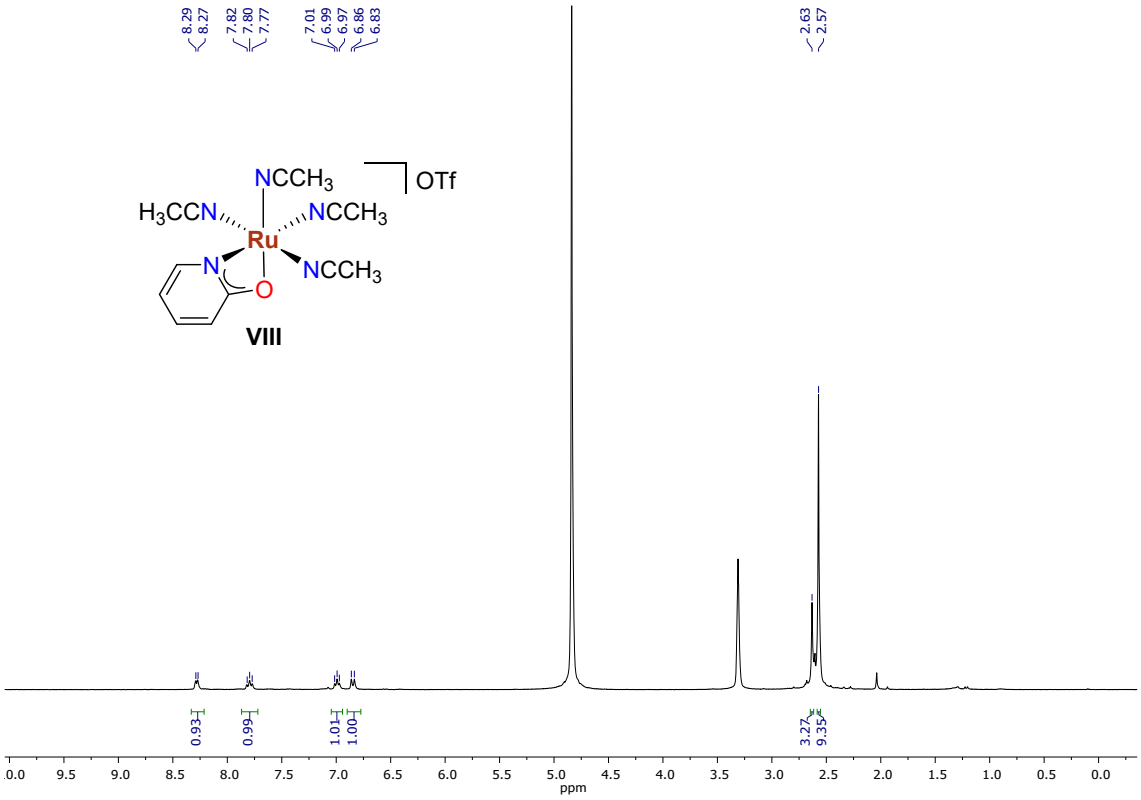

Figure S34 ^{1}H NMR spectrum of **VIII** in MeOD. Signals at 4.87 and 3.31 ppm correspond to water and MeOD respectively.

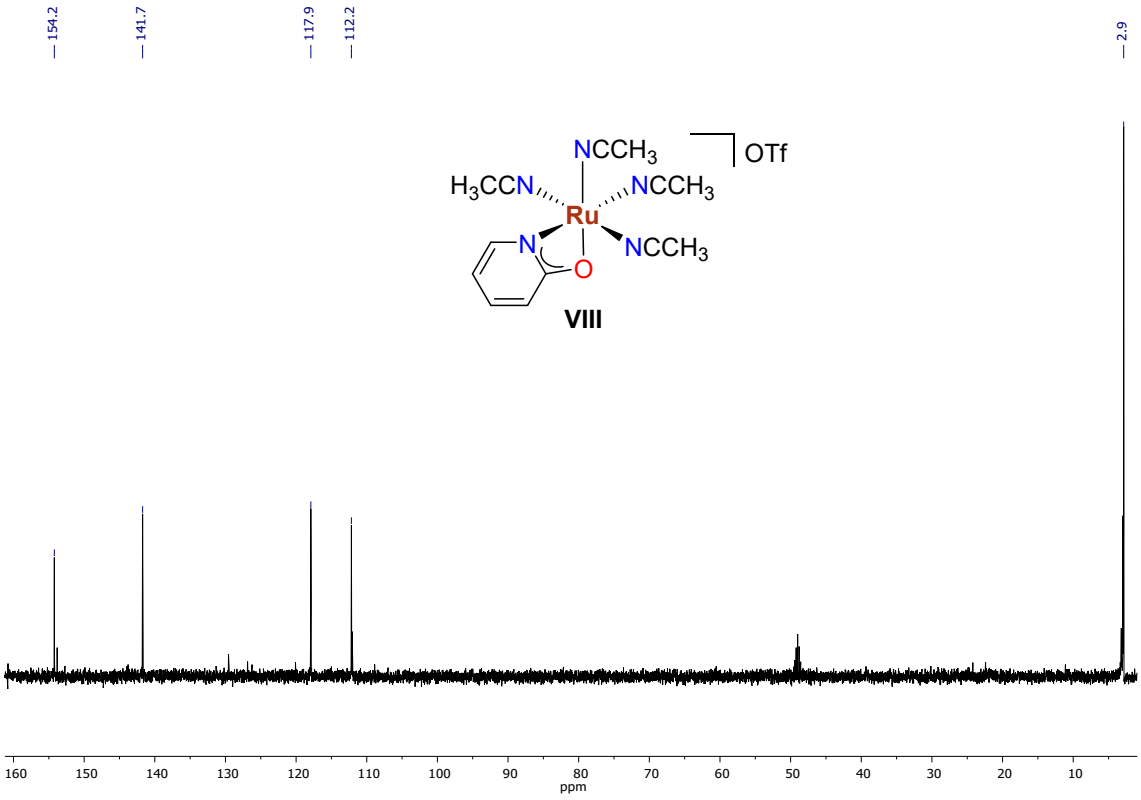

Figure S35 ^{13}C NMR of complex **VIII** in MeOD.

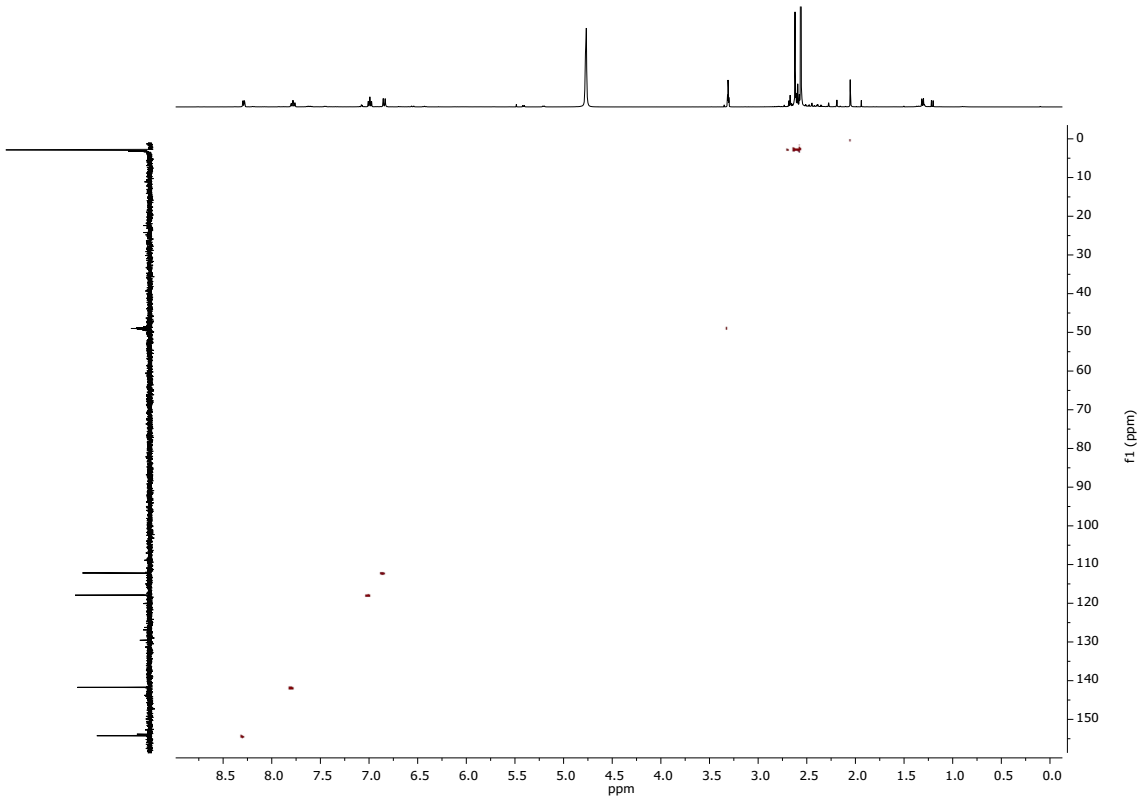

Figure S36 ^{1}H-^{13}C HSQC of complex **VIII** in MeOD.

HR-MS of complex VIII

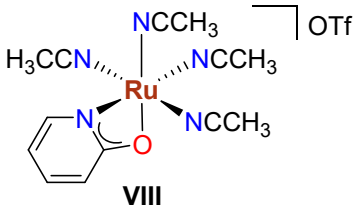

VIII

MW: 508.44 g/mol ($[RuC_{13}H_{16}N_5O]CF_3SO_3$)

Fragment: 319.0143 $[M - OTf - MeCN]^+$
277.9868 $[M - OTf - 2MeCN]^+$
236.9609 $[M - OTf - 3MeCN]^+$

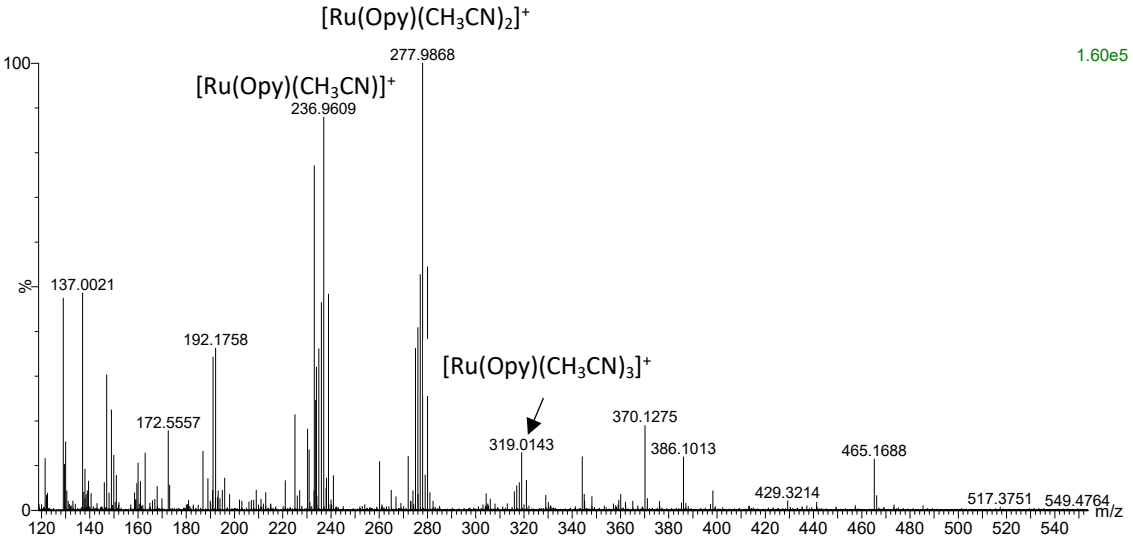

Figure S37 HR-MS of complex **VIII** in MeOH.

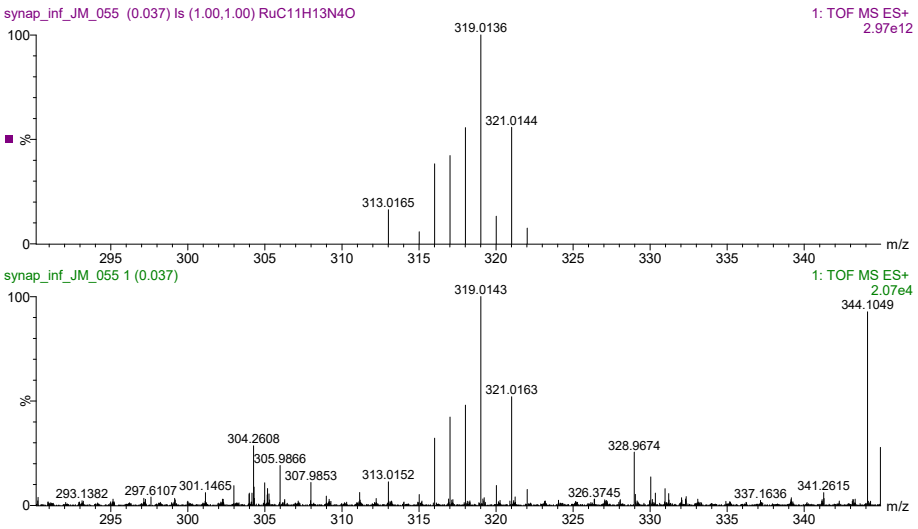

Figure S38 Comparison of simulated (top) and experimental (bottom) HR-MS of complex **VIII.**

UV-Vis Absorption spectrum of complex VIII

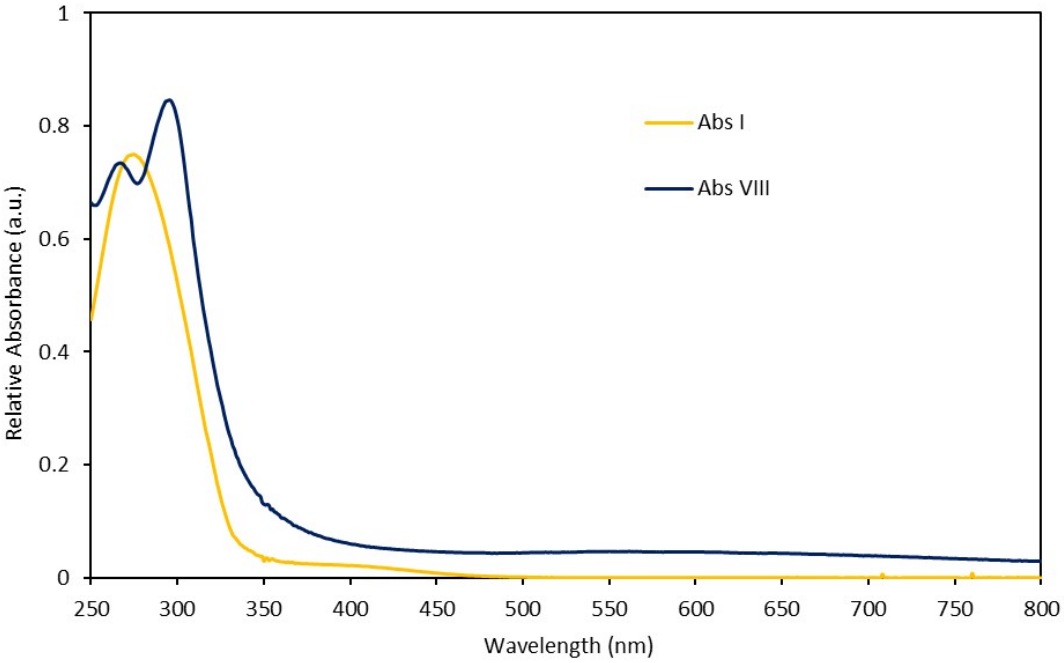

Figure S39 Absorption spectra of complexes **I** *vs* **VII** in degassed methanol (5.0 x 10^{-5} M).

S3. Photocatalytic dehydrogenation reactions

S3.1. General procedure for photocatalytic reactions

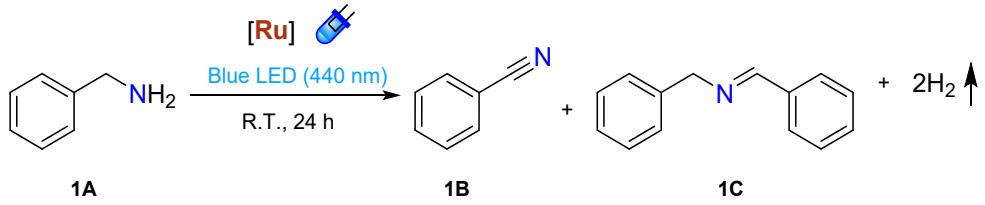

In a generic catalytic reaction, 0.3 mmol of benzylamine, 3.0 mol% of the required catalyst and 0.2 mmol of 1,3,5-trimethoxybenzene (internal standard) were dissolved in 1.0 mL of dry methanol. Reaction was placed in a 12 mL Schlenk flask connected to a bubbler filled with mineral oil (the bubbler allows the release of hydrogen gas and excludes air from the reaction system). Then, reactions were left at room temperature in a homemade photoreactor (Fig. S40) using 45 W Kessil PR160L blue LEDs (λ = 440 nm) lamps placed at the distance of 5 cm of the centre of the Schlenk (intensity of 172 mW/cm^2) and a fan for the tabulated time. Before and after reaction, an aliquot was extracted and analysed by GC-FID to obtain conversions and yields (See S3.2 section).

a)

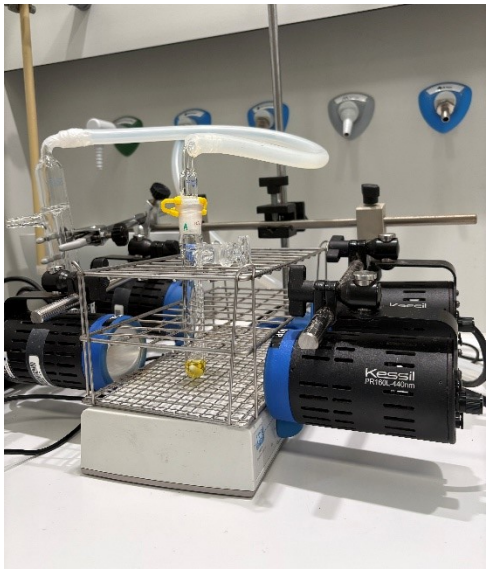

b)

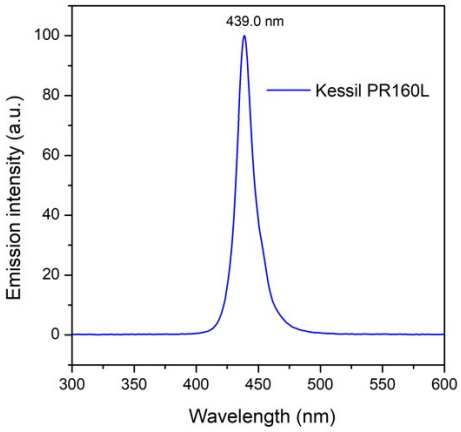

Figure S40 (a) Photoreactor system and (b) emission spectrum of Kessil PR160L-440 nm lamp.

S3.2. GC-FID Quantification

GC-FID Quantification was performed using an Agilent 8890GC System equipped with an Agilent 123-103B Column. Temperature program: 1) 80 °C, 10 °C/min until 150 °C, hold 1 min. 2) 150 °C, 20 °C/min until 270 °C, hold 2 min. Total time: 16 min.

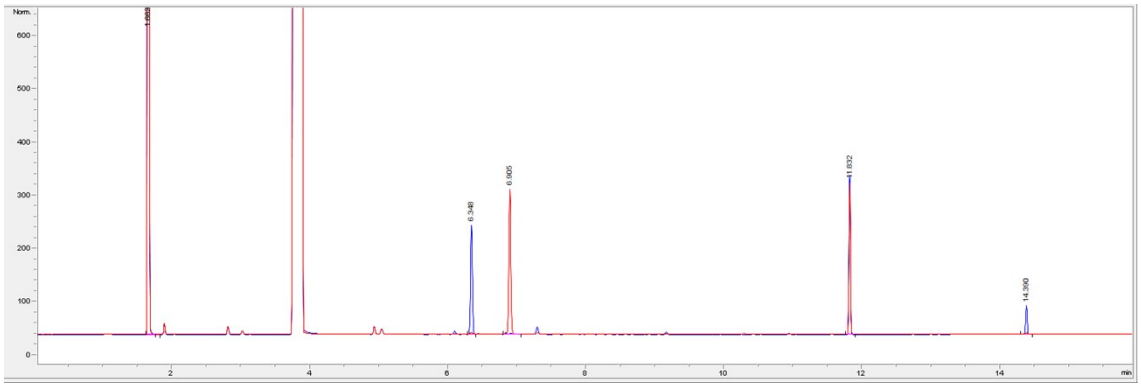

Figure S41 Representative reaction progress by GC/FID in the ADH of benzylamine (r.t. = 6.91 min) to benzonitrile (r.t. = 6.35 min) and N-benzylidenebenzylamine (r.t.= 14.39 min) in the presence of 0.2 mmol of 1,3,5-trimethoxybenzene as an internal standard (r.t. = 11.84 min). Red line: 0h; blue line: 24h.

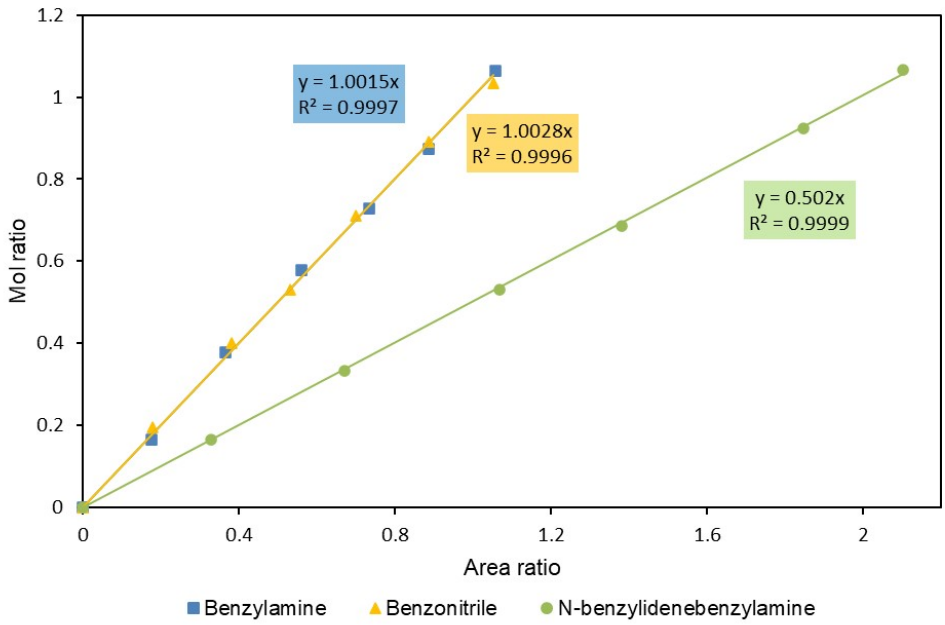

Figure S42 Calibration curves of benzylamine (blue), benzonitrile (orange) and N-benzylidenebenzylamine (green).

To quantify the obtained products, we generated calibration curves using 1,3,5-trimethoxybenzene as an internal standard (Fig. S42). Solutions with known concentrations of the amine, nitrile, imine and internal standard were prepared, and measurements were performed by GC-FID. The moles of product were calculated using the slope of the curve, the

moles of standard (n_{st}) and the area ratio between the product (A_P) and the standard (A_{st}) using the following equation:

$$n_P = slope \times \left(\frac{A_P}{A_{st}} \times n_{st}\right)$$

$n_P = moles\ of\ product$
$A_P = Area\ of\ product$
$A_{st} = Area\ of\ standard$
$n_{st} = moles\ of\ standard$

Once the moles of products and reactants were obtained, the percentages of conversion, yields and selectivity could be calculated with the following equations:

$$\%Conv = \frac{n_{R,\ initial} - n_{R,\ final}}{n_{R,\ initial}} \times 100\ , \qquad \%Yield = \frac{n_P \times s_F}{n_{R,\ initial}} \times 100$$

$$\%Select = \frac{n_P \times s_F}{n_{R,\ initial} - n_{R,\ final}} \times 100$$

$n_R = moles\ of\ reactant$
$n_P = moles\ of\ product$
$s_F = Stoichiometric\ factor$

S3.3. General procedure for scope reactions

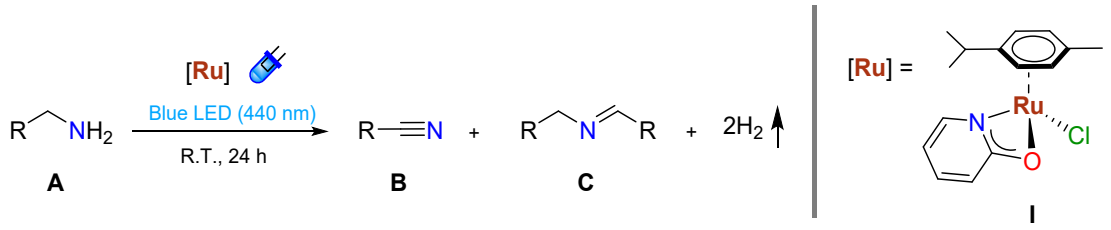

A mixture containing the corresponding amine (0.3 mmol), catalyst **I** (3.0 mol%), 0.2 mmol of TMB (internal standard), deoxygenated MeOH (1.0 mL), and a PTFE-coated magnetic bar were placed in a 12 mL Schlenk flask connected to a bubbler filled with mineral oil. The photocatalytic reactions were carried out using 45 W Kessil PR160L blue LEDs (λ = 440 nm) lamps placed at the distance of 5 cm of the centre of the Schlenk (intensity of 172 mW/cm^2) at room temperature (see Fig. S40) for 24 h. Before and after reaction, an aliquot was extracted and analysed by GC-FID. Calibration curve of each amine and nitrile was obtained to calculate conversions and yields. Nitriles 1B and 8B were purified by silica gel chromatography (h: 10 cm; Ø :1 cm) using 90:10 pentane: diethylether mixture and were characterised by NMR spectroscopy.

S3.4. ^{1}H NMR spectra of nitrile derivatives

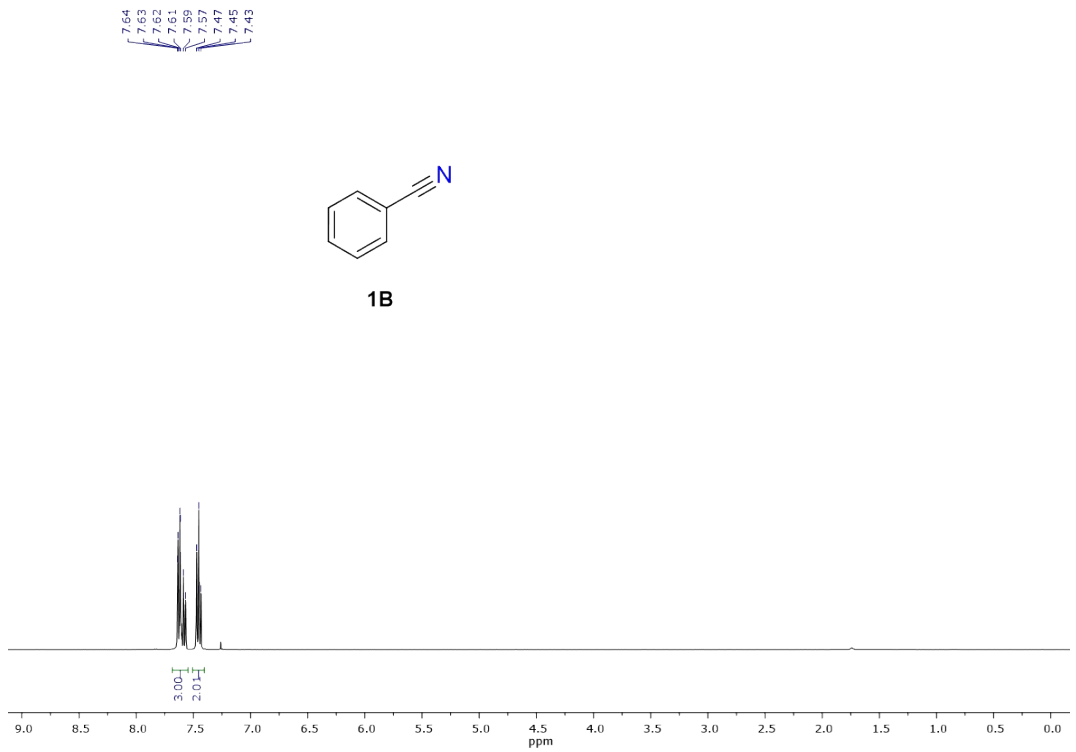

Figure S43 ^{1}H NMR spectrum (400 MHz) of benzonitrile **1B** in $CDCl_3$ after 24h of reaction and purification by column chromatography.

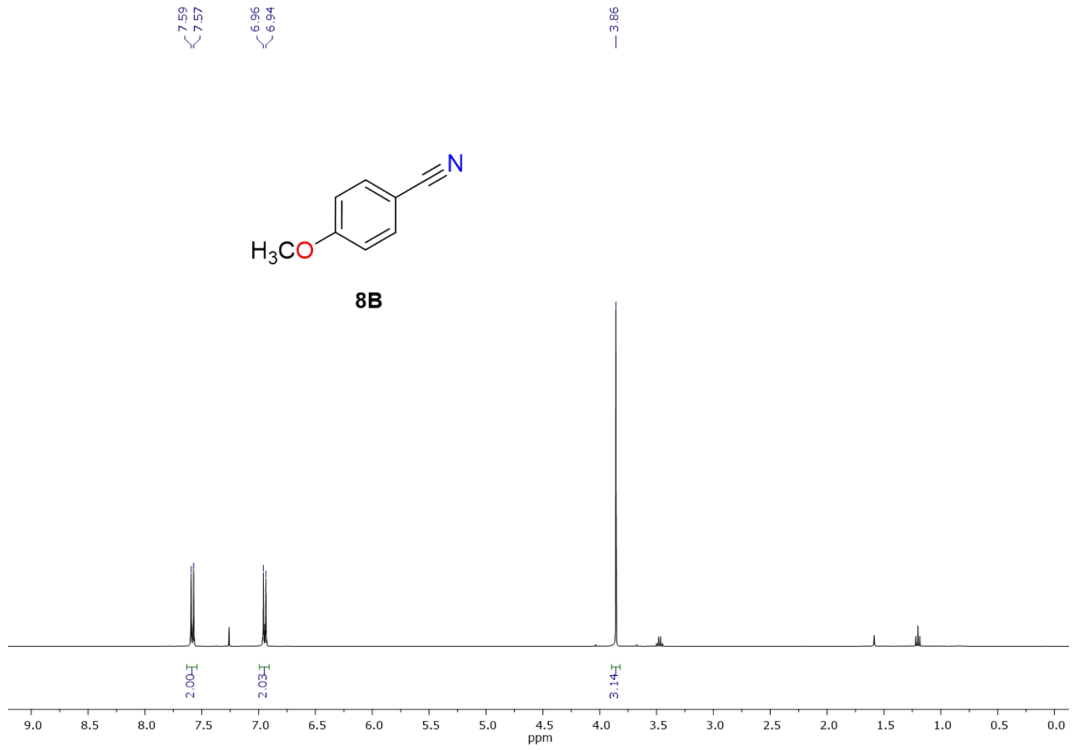

Figure S44 ^{1}H NMR spectrum (400 MHz) of 4-methoxybenzonitrile **8B** in $CDCl_3$ after 24h of reaction and purification by column chromatography.

S4. Mechanistic insights

S4.1. Detection of molecular hydrogen

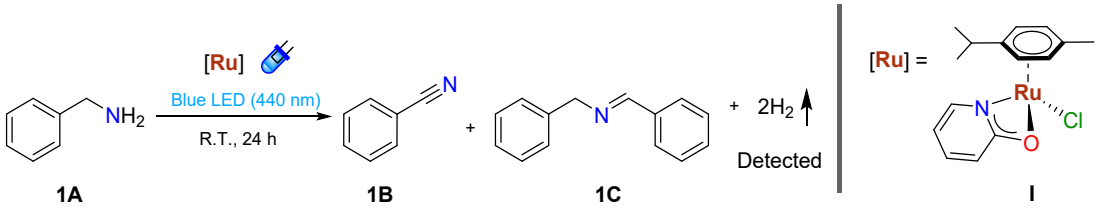

To detect hydrogen, the reaction was scaled up: 1.5 mmol of benzylamine and 3.0 mol% of catalyst **I** were dissolved in 3.0 mL of dry methanol. Reaction was placed in a 50 mL Schlenk flask sealed with a rubber septum and parafilm. Then, it was left at room temperature in a home-made photoreactor (see Fig. S40) for 20h. After reaction, the internal gas phase was analysed by Gas Chromatography (GC-TCD) analysis (Agilent 990 Micro-GC gas chromatograph) using argon as carrier gas. To do that, a sealed vial connected to a continuous flow of argon was used. In this vial, we connected the GC-TCD entry system, which has a syringe that absorbs a certain volume of the headspace directly to the column to obtain the chromatogram (Fig. S45). We purged the system three times to ensure that there is no other gas present in the vial. Then, we connected the vial to the reaction using a cannula to obtain the chromatogram of the internal headspace of the reaction. GC-TCD spectrum clearly confirmed the formation of molecular hydrogen from the reaction (Fig. S46). Conversion of the reaction was 6%, indicative of the slower reaction times achieved when hydrogen cannot be released from the reaction media.

Figure S45 Experimental set-up used to detect hydrogen by GC-TCD.

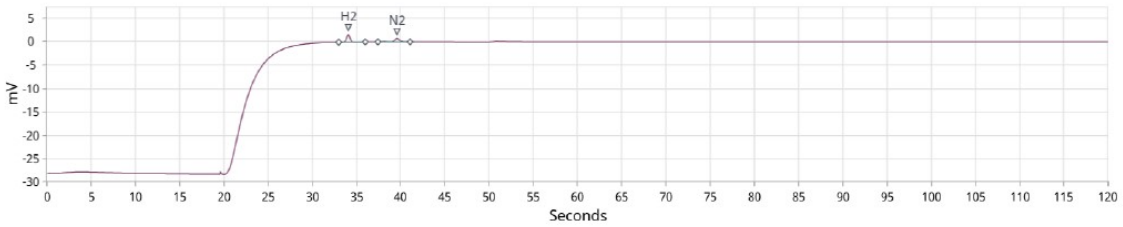

Figure S46 GC-TCD spectrum of the internal gas phase (containing H_2 and N_2) after 20h of reaction in the photodehydrogenation of benzylamine using catalyst **I**.

S4.2. Kinetic studies: Order in catalyst

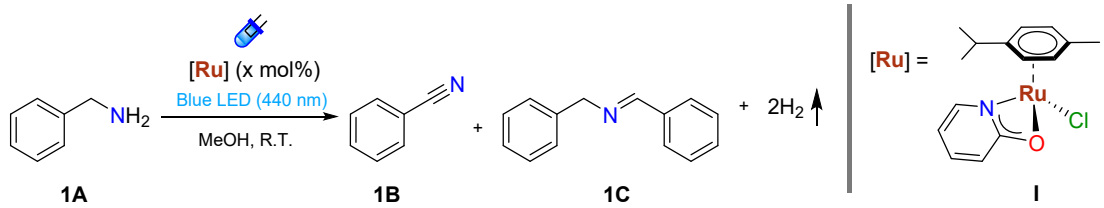

To obtain the reaction progress profiles, 0.3 mmol of benzylamine, a certain amount of catalyst **I** (x mol%) and 0.2 mmol of 1,3,5-trimethoxybenzene (internal standard) were dissolved in 1.0 mL of dry methanol. Reaction was placed in a 12 mL Schlenk flask connected to a bubbler filled with mineral oil. Then, reactions were left at room temperature in a homemade photoreactor (Fig. S40) using 45 W Kessil PR160L blue LEDs (λ = 440 nm) lamps placed at the distance of 5 cm of the centre of the Schlenk (intensity of 172 mW/cm^2) and a fan. At selected times, an aliquot was extracted and analysed by GC-FID to obtain conversions and selectivity (Fig. S47 - S48).

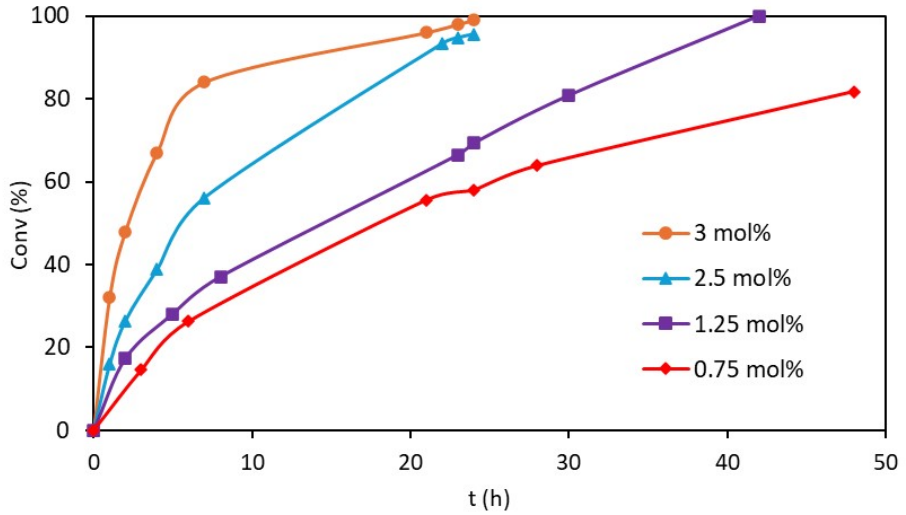

Figure S47 Kinetic profile of the photocatalytic dehydrogenation of benzylamine at different catalyst loadings of complex **I**. Conversions determined by GC-FID using TMB as internal standard.

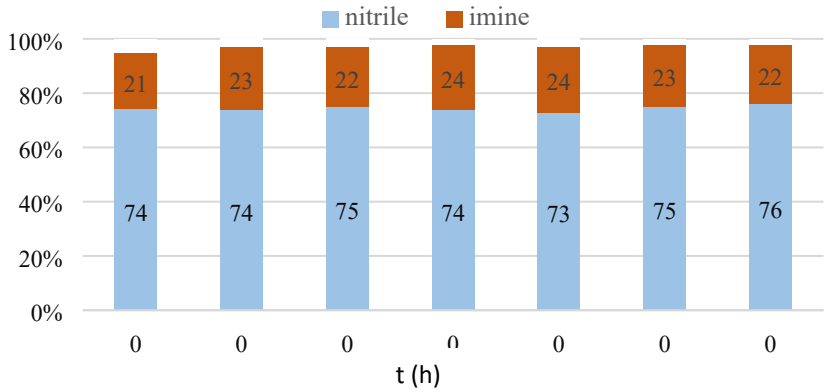

Figure S48 Product selectivity of nitrile / imine in the photocatalytic dehydrogenation of benzylamine using catalyst **I** at 3.0 mol% catalyst loading.

Order in catalysts was stablished using graphical analysis based on the normalized time scale method (VTNA) [8–10].

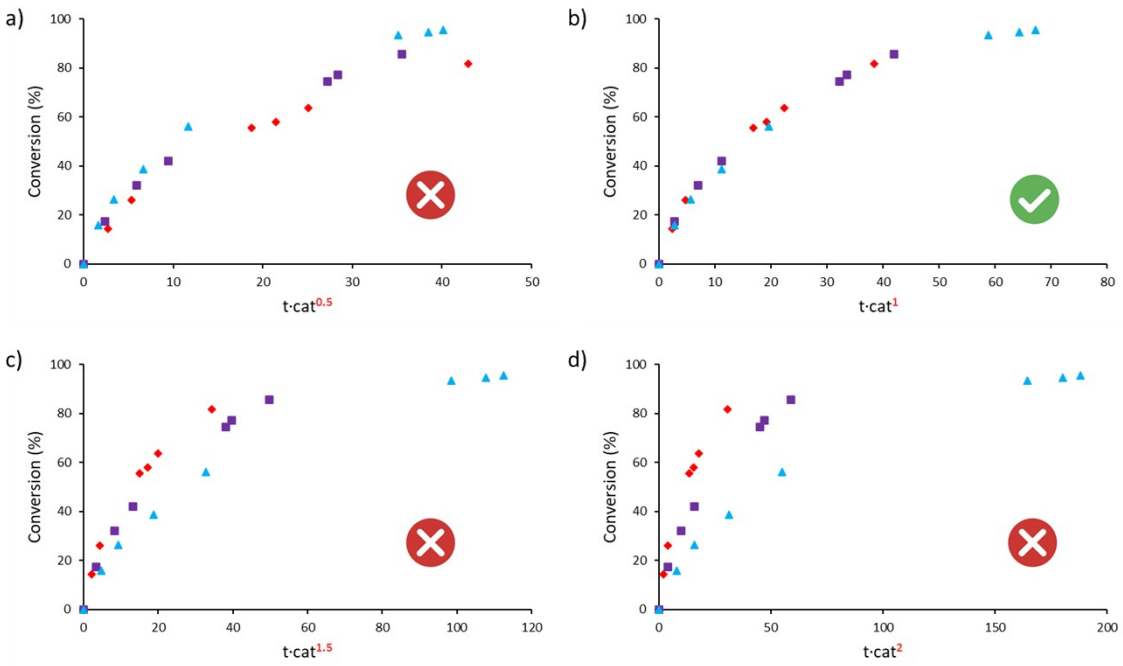

Figure S49 Evaluation of order in catalyst using variable time normalization analysis (VTNA). Order in catalyst corresponds to the representation showing the greatest overlay according to VTNA, which is 1 in this case. Data: blue triangles (2.5 mol%), purple squares (1.25 mol%) and red diamonds (0.75 mol%).

S4.3. Monitoring of the reaction by ^{1}H NMR spectroscopy

^{1}H NMR monitoring of the reaction was obtained by dissolving *p*-methoxybenzylamine (0.3 mmol) and catalyst **I** (3.0 mol%) in 1.0 mL of deuterated methanol. Reaction was placed in a 12 mL Schlenk flask connected to a bubbler filled with mineral oil. Then, reaction was left at room temperature in a homemade photoreactor (Fig. S36). At selected times, a 0.5 mL aliquot was extracted, analysed by ^{1}H NMR spectroscopy, and returned to the reaction Schlenk until completion of the reaction (Fig. S50).

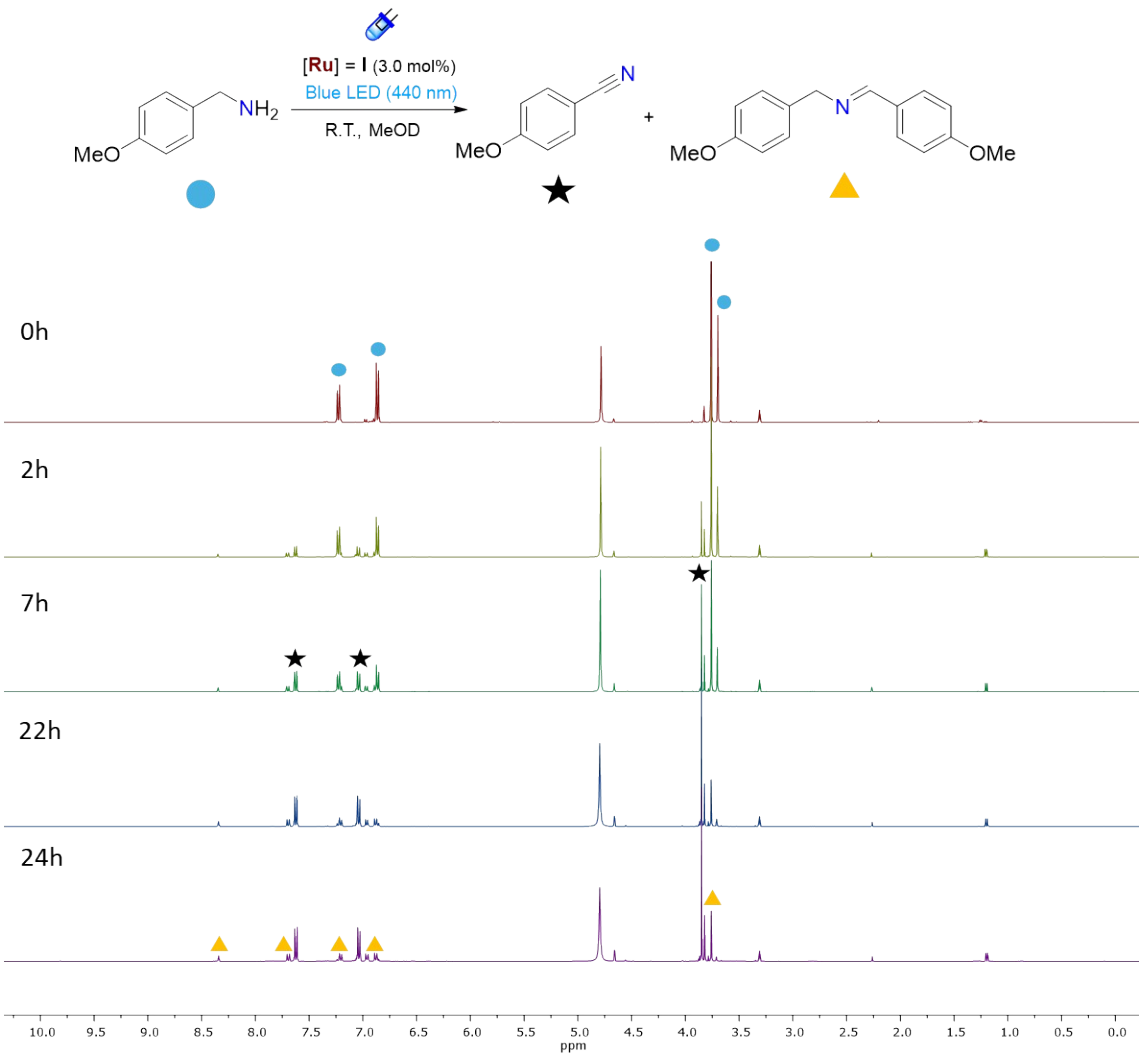

Figure S50 Monitoring of the reaction by ^{1}H NMR spectroscopy using MeOD.

S4.4. Pseudocatalytic experiment

p-methoxybenzylamine (3.7 µL, 0.028 mmol) and catalyst **I** (5 mg, 0.014 mmol) were dissolved in 1.0 mL of deuterated methanol. Reaction was placed in an NMR tube opened to the atmosphere using a bubbler. Then, reaction was left at room temperature in a homemade photoreactor (Fig. S40). At selected times, NMR tube was closed under inert atmosphere and analysed by ^{1}H NMR spectroscopy (Fig. S51).

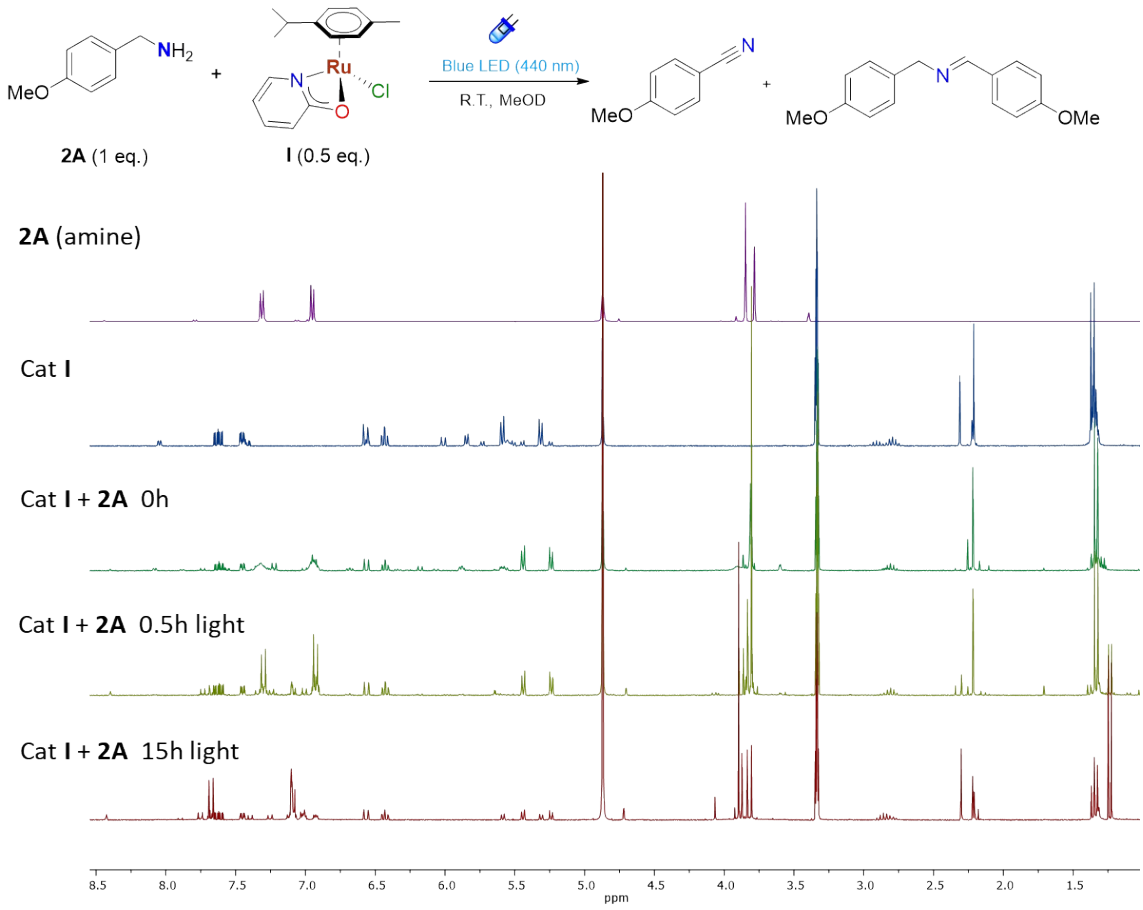

Figure S51 Pseudocatalytic experiment using 1 eq. of *p*-methoxybenzylamine and 0.5 eq. of catalyst **I** in MeOD.

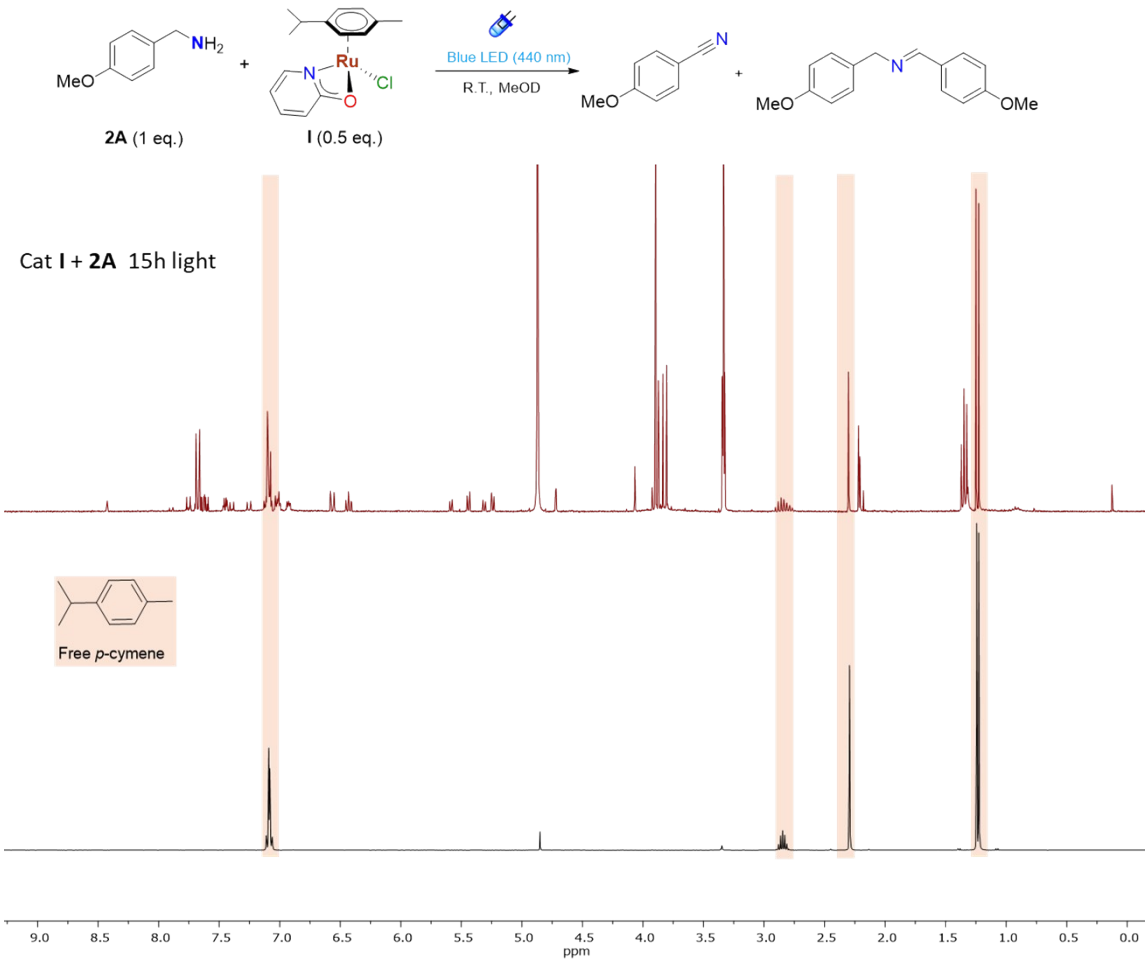

Figure S52 Comparison of the pseudocatalytic reaction after 15h of blue light *vs* commercial free *p*-cymene.

S4.5. Catalyst stability

5 mg of complex **I** were dissolved in 1.0 mL of dry MeOD under inert atmosphere (standard conditions). Solution was irradiated with blue light (440 nm, see Fig. S40) during 16h. An aliquot of 0.5 mL was extracted at selected times to obtain ^{1}H NMR spectra (Fig. S53).

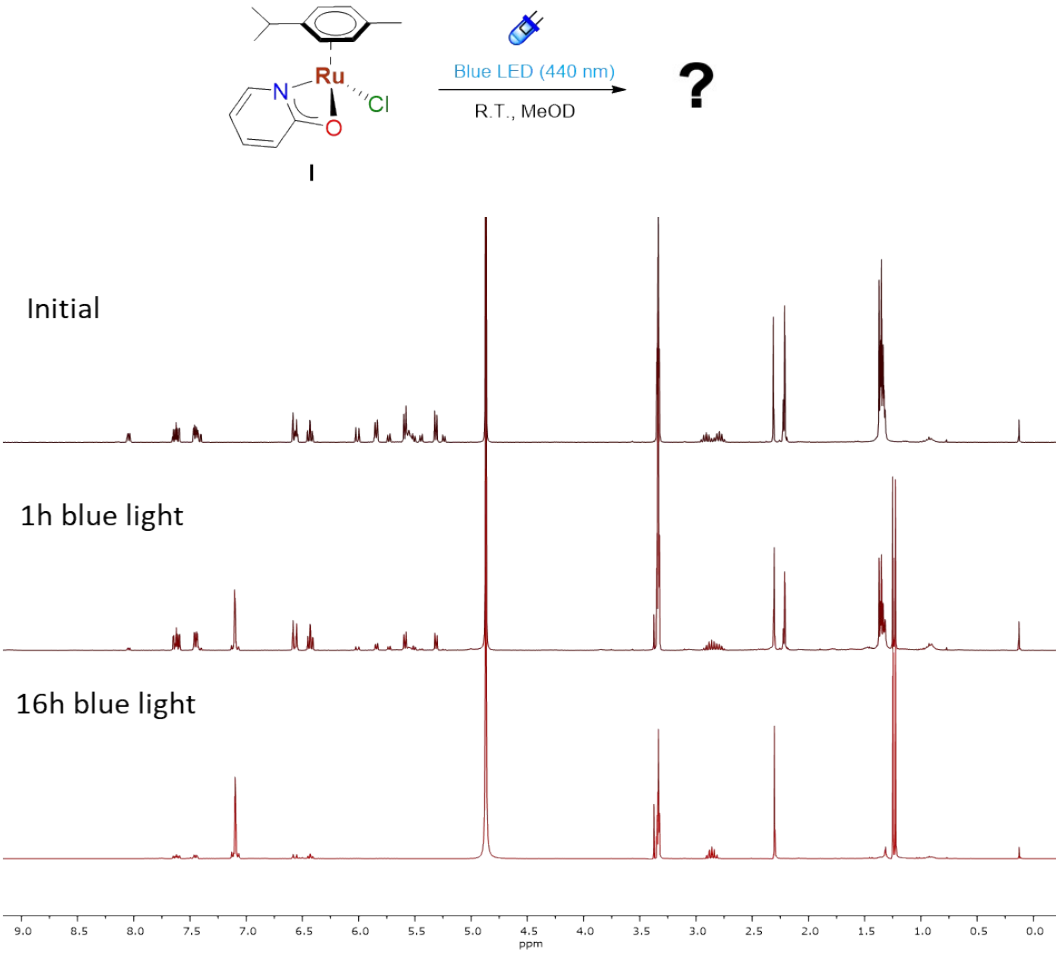

Figure S53 Catalyst stability experiment. Solution of complex **I** in MeOD was irradiated under blue light (λ= 440 nm). ^{1}H NMR spectra were recorded after 1h and 16h of blue light irradiation. After 16h the dissociation of free *p*-cymene was observed (signals at 7.1, 2.7 and 1.2 ppm).

Figure S54 Reaction image before (a) and after 24h (b) of light irradiation. A drastic change in the reaction color was observed, changing from yellow to dark brown.

S4.6. UV-Vis kinetic experiment

To perform UV-Vis kinetic experiment, 9 x 10^{-3} mmol of complex **I** were diluted in 1 mL of MeOH (standard conditions). Then, 0.3 mmol of benzylamine were added. The mixture is irradiated at 440 nm for the selected time (0.5h, 1h, 1.5h, 3h, 4h, 8h). For UV-Vis measurements, a 200 µL aliquot is extracted, diluted to 4 mL and measured directly in the UV-Vis spectrometer.

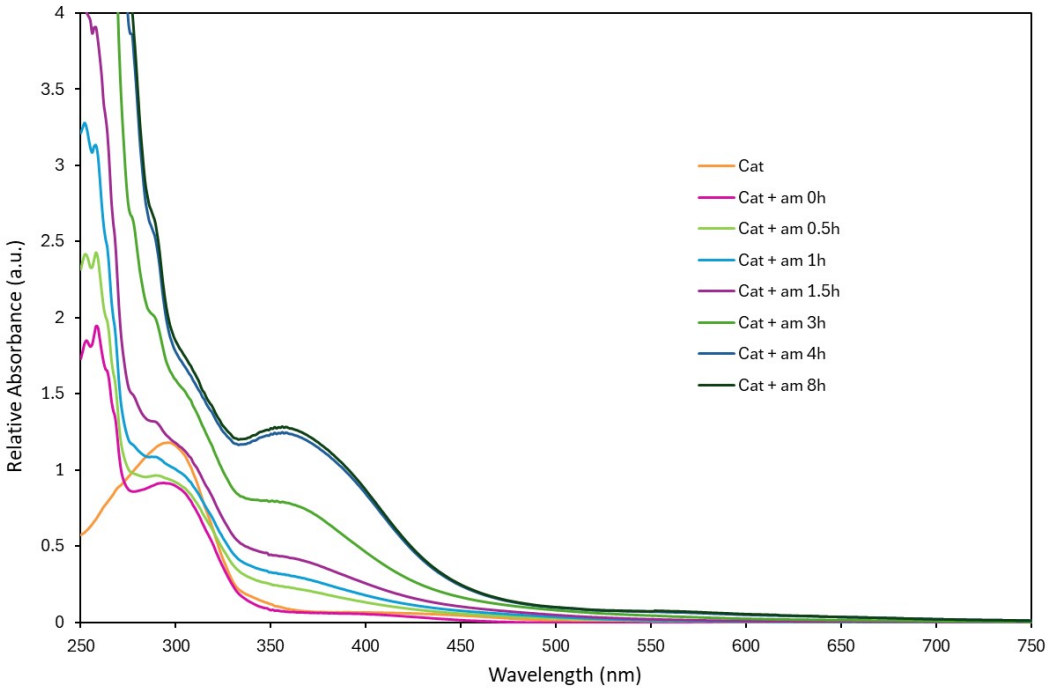

Figure S55 Absorption spectra of complex **I**, and a mixture of complex **I** + benzylamine before and after applying light irradiation (440 nm) in degassed methanol. The appearance of a new band in the blue region of absorption spectra could be seen after light irradiation.

S4.7. Poisoning experiments and filtration experiment

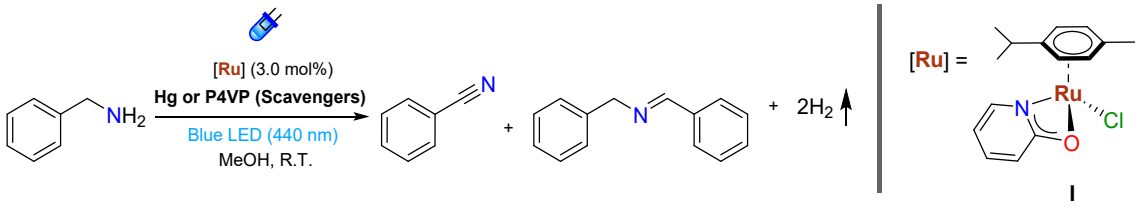

Poisoning experiments using P4VP (poly(4-vinylpyridine)) as a scavenger of molecular species and the Hg drop test as a scavenger of nanoparticles were performed. Scavengers were added before the reaction started, and the reaction was performed using benzylamine as substrate under standard conditions. During the reaction, aliquots at selected times were extracted and analysed by GC-FID to obtain conversions and compared to the reaction without scavenger (Fig. S56).

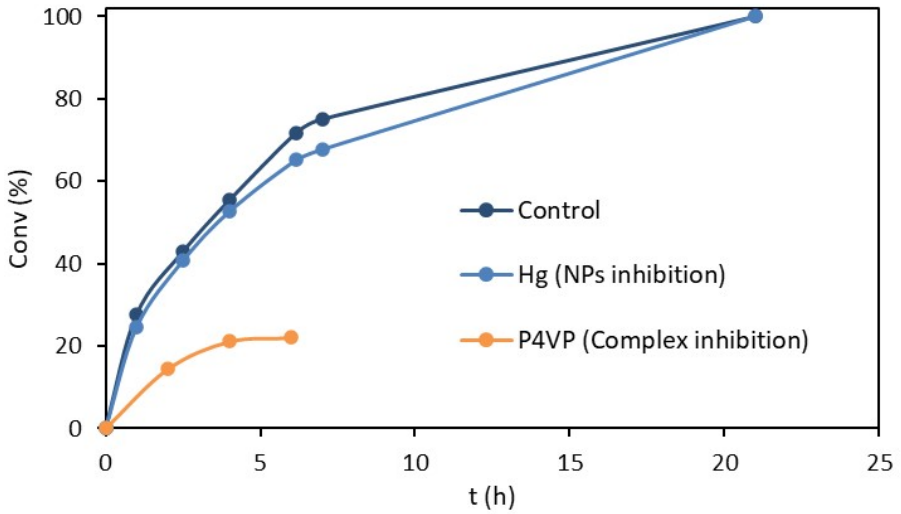

Figure S56 Poisoning experiments in the photodehydrogenation of benzylamine catalysed by **I**. P4VP (poly-(4-vinylpyridine)) was added as molecular species scavenger (orange line) or Hg (mercury test) was used as a scavenger of NPs (light blue line).

Additionally, a filtration experiment was performed to check if Ru heterogeneous species are formed during the catalytic reaction. To do that, reaction monitoring of the photodehydrogenation of benzylamine under standard conditions was performed. After 4 hours, catalytic reaction was cannulated through a celite pad. Then, the filtrated solution was further monitored until completion. No significant changes compared to the reaction without filtration were observed, supporting its homogeneous nature (Fig. S57).

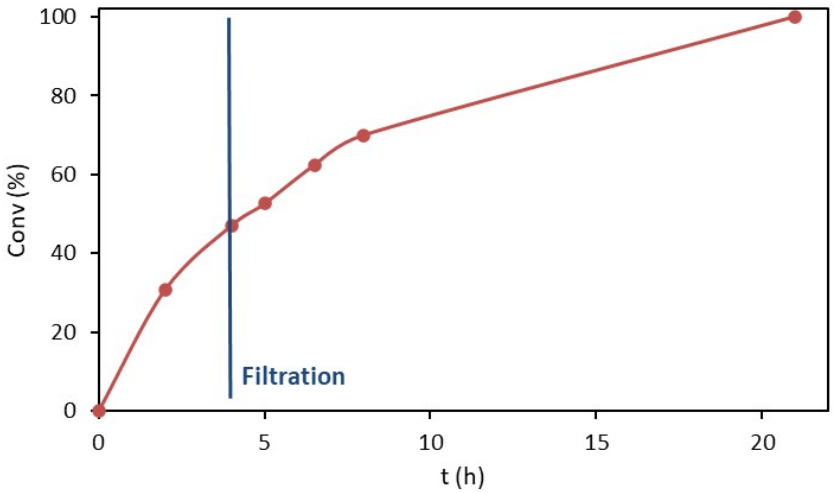

Figure S57 Monitoring of the photodehydrogenation of benzylamine using complex **I** under standard conditions. After 4h, reaction was filtered and monitored again under blue light until completion.

S4.8. Comparison of catalytic activity of complex I vs VIII

Table S1 Photocatalytic activity of complex **I** *vs* complex **VIII**.

	Cat (mol%)	Conv(%)	Selectivity (%)	
			Nitrile	Imine
1	**I** (3.0 mol%)	**100**	76	22
2	$[Ru(Opy)(CH_3CN)_4]OTf$ **VIII** (3.0 mol%)	**100**	70	28

S4.9. ESI-MS Experiments

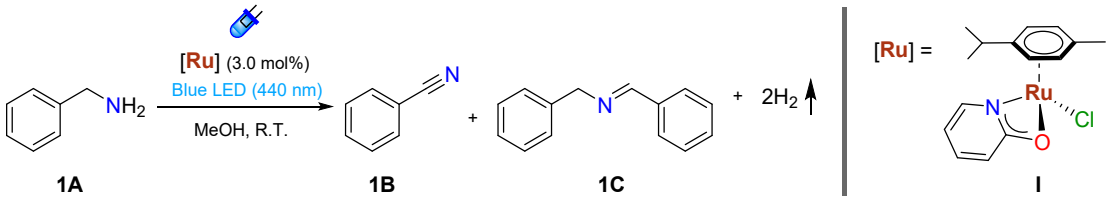

To perform ESI-MS experiments, 0.3 mmol of benzylamine and 3.0 mol% of catalyst **I** were dissolved in 1.0 mL of dry methanol. Reaction was placed in a 12 mL Schlenk flask connected to a bubbler filled with mineral oil (the bubbler allows the release of hydrogen gas and excludes air from the reaction system). Then, reaction was left at room temperature in a homemade photoreactor (Fig. S40) using blue LEDs (λ= 440 nm). Before and after 2h of reaction, an aliquot was extracted and analysed by ESI-MS spectrometry (Fig. S58 – S59).

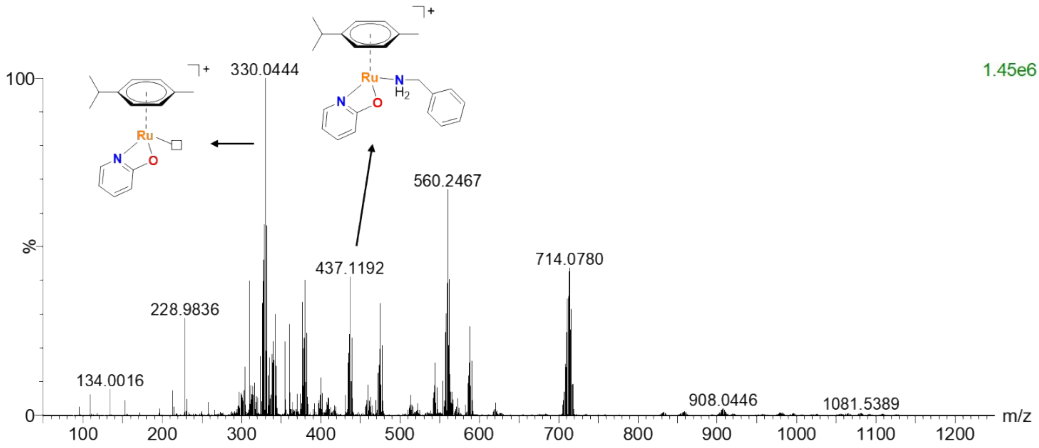

Figure S58 ESI-MS spectrum obtained after mixing 0.3 mmol of benzylamine and 3.0 mol% of catalyst **I** in 1.0 mL of MeOH (before light irradiation).

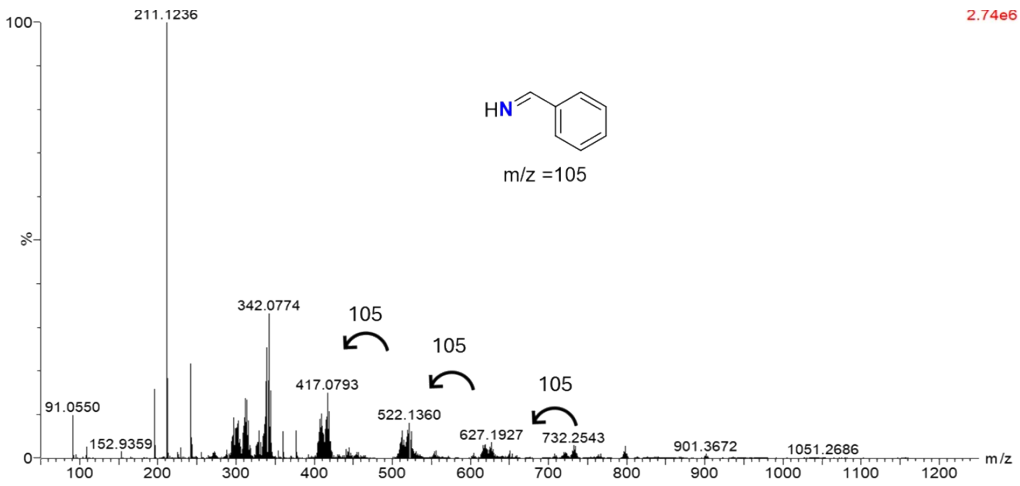

Figure S59 ESI-MS spectrum obtained after 2h of light irradiation of a mixture containing 0.3 mmol of benzylamine and 3.0 mol% of catalyst **I** in 1.0 mL of MeOH.

S4.10. Hydride trapping experiment

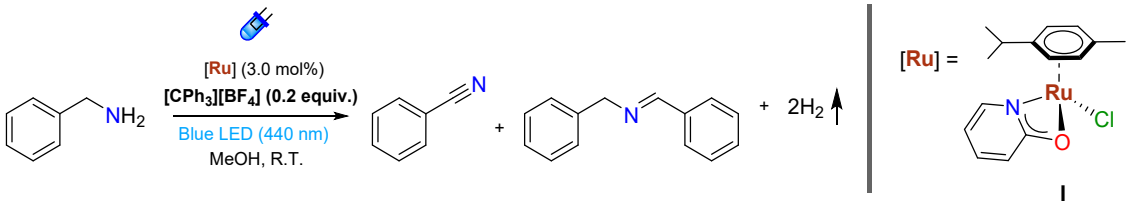

I

Benzylamine (0.3 mmol), Ru catalyst **I** (3.0 mol%)**,** tritylium tetrafluoroborate (0.06 mmol, 0.2 equiv.) and 1,3,5-trimethoxybenzene (0.2 mmol, used as internal standard) were dissolved in 1.0 mL of dry methanol. Reaction was placed in a 12 mL Schlenk flask connected to a bubbler filled with mineral oil (the bubbler allows the release of hydrogen gas and excludes air from the reaction system). Then, reaction was left at room temperature in a homemade photoreactor (Fig. S40) using 45 W Kessil PR160L blue LEDs (λ = 440 nm) lamps placed at the distance of 5 cm of the centre of the Schlenk (intensity of 172 mW/cm^2) and a fan for the tabulated time. During the reaction, aliquots at selected times were extracted and analysed by GC-FID to obtain conversions and yields (Fig. S60).

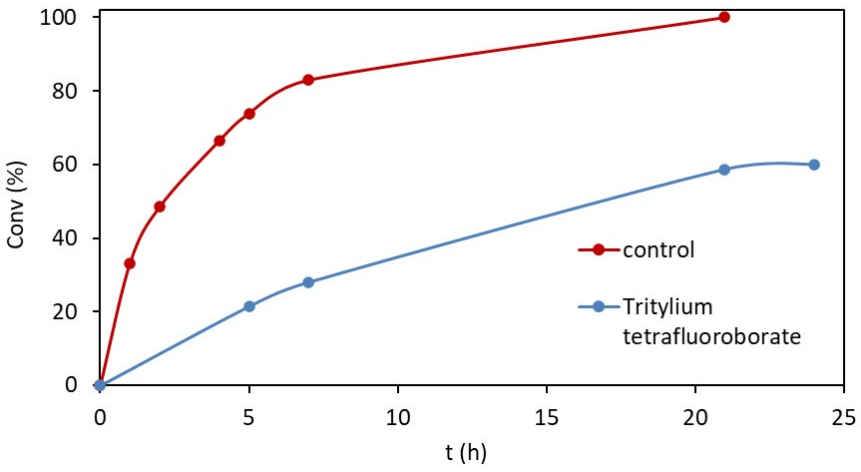

Figure S60 Kinetic profile of the photocatalytic dehydrogenation of benzylamine with tritylium tetrafluoroborate as hydride scavenger (blue) and control (red).

S5. References

(1) Lahuerta, P.; Latorre, J.; Sanaú, M.; Cotton, F. A.; Schwotzer, W. Synthesis of Ruthenium (II) Compounds with Ortho-Oxypyridinate Ligands (Hp). Crystal Structure Characterization of [Ru(N6-p-CH3C6H4CH(CH3)2)Cl(Hp)]. *Polyhedron* 1988, **7** (14), 1311–1316. https://doi.org/https://doi.org/10.1016/S0277-5387(00)81229-2.

(2) Sahli, Z.; Sundararaju, B.; Achard, M.; Bruneau, C. Selective Carbon-Carbon Bond Formation: Terpenylations of Amines Involving Hydrogen Transfers. *Green Chem.* 2013, **15** (3), 775–779. https://doi.org/10.1039/c3gc36982j.

(3) Nongbri, S. L.; Therrien, B.; Rao, K. M. Reactivity Study of Arene(Azido)Ruthenium N∩O-Base Complexes with Activated Alkynes. *Inorg. Chim. Acta* 2011, **376** (1), 428–436. https://doi.org/10.1016/j.ica.2011.07.004.

(4) Nieto, I.; Livings, M. S.; Sacci, J. B.; Reuther, L. E.; Zeller, M.; Papish, E. T. Transfer Hydrogenation in Water via a Ruthenium Catalyst with OH Groups near the Metal Center on a Bipy Scaffold. *Organometallics,* 2011, **30** (23), 6339–6342. https://doi.org/10.1021/om200638p.

(5) Sabater, S.; Mata, J. A.; Peris, E. Catalyst Enhancement and Recyclability by Immobilization of Metal Complexes onto Graphene Surface by Noncovalent Interactions. *ACS Catal.,* 2014, **4** (6), 2038–2047. https://doi.org/10.1021/cs5003959.

(6) Mejuto, C.; Ibáñez-Ibáñez, L.; Guisado-Barrios, G.; Mata, J. A. Visible-Light-Promoted Iridium(III)-Catalyzed Acceptorless Dehydrogenation of N-Heterocycles at Room Temperature. *ACS Catal.,* 2022, **12** (10), 6238–6245. https://doi.org/10.1021/acscatal.2c01224.

(7) Strydom, I.; Guisado-Barrios, G.; Fernández, I.; Liles, D. C.; Peris, E.; Bezuidenhout, D. I. A Hemilabile and Cooperative N-Donor-Functionalized 1,2,3-Triazol-5-Ylidene Ligand for Alkyne Hydrothiolation Reactions. *Chem. - Eur. J.,* 2017, **23** (6), 1393–1401. https://doi.org/10.1002/chem.201604567.

(8) Nielsen, C. D. T.; Burés, J. Visual Kinetic Analysis. *Chem. Sci.,* 2019, **10** (2), 348–353. https://doi.org/10.1039/C8SC04698K.

(9) Burés, J. A Simple Graphical Method to Determine the Order in Catalyst. *Angew. Chem. Int. Ed.,* 2016, **55** (6), 2028–2031. https://doi.org/10.1002/anie.201508983.

(10) Martínez-Carrión, A.; Howlett, M. G.; Alamillo-Ferrer, C.; Clayton, A. D.; Bourne, R. A.; Codina, A.; Vidal-Ferran, A.; Adams, R. W.; Burés, J. Kinetic Treatments for Catalyst Activation and Deactivation Processes Based on Variable Time Normalization Analysis. *Angew. Chem. Int. Ed.,* 2019, **58** (30), 10189–10193. https://doi.org/10.1002/anie.201903878.